Three dimensional shape modeling of human body in various postures by light stripe triangulation

Takuya Funatomi

March 2007

Abstract

In this thesis, we discuss human body modeling of individual based on light stripe triangulation as three-dimensional shape measurement.

Light stripe triangulation is one of the most frequently used methods of three-dimensional shape measurement since the method can measure the detailed shape accurately even if the subject has no texture. However, the method has three disadvantages as follows. The first disadvantage is 'incompleteness'. Light stripe triangulation projects a laser sheet onto the subject. We can calculate the three-dimensional shape of the illuminated part of the subject by observing it with calibrated camera(s). Therefore, we cannot measure the part where has never been projected the laser sheet or visible to the camera directly due to occlusion. The second disadvantage is 'time consuming'. In light stripe triangulation, we need to scan the whole subject with the laser sheet in order to acquire full shape. Therefore, it takes a certain time for scanning to perform the measurement. If the subject moves during the scanning, the accuracy would be degraded since the acquired shape is distorted due to the subject's motion. The third disadvantage is 'discreteness'. In light stripe triangulation, the shape of the subject is acquired as a number of points, which is termed point-cloud, which are placed on the subject's surface in three-dimensional space. Since such point-cloud does not represent the surface explicitly, it is necessary to reconstruct the surface by making connectivity among the points. Although several methods have been proposed to reconstruct surface for point-cloud of general object, superfluous surface which covers the convex area would be constructed with such methods from the point-cloud of human body which is incomplete and non-uniformly distributed and forms complex shape.

In conventional human body modeling, it is supposed that the subject makes an effort to maintain the standing posture during the measurement. Under this supposition, it is assumed that the shape of subject is roughly

known, and the subject is treated as a stationary rigid object during the measurement for tackling the disadvantages in light stripe triangulation. The incompleteness disadvantage is tackled by assuming that the subject makes the standing posture with holding arms and legs away from the body in order to minimize the occluded part. The time consuming disadvantage is tackled by assuming that the subject can stay still as to be stationary rigid object in such stable posture for a short time. For supporting the assumption, several methods have been proposed to shorten the time of measurement. The discreteness disadvantage is tackled by assuming that the shape of the subject is roughly known since the subject will make the particular posture.

However, all disadvantages are not completely overcome even if we assume that the subject maintains the standing posture during the measurement. As to incompleteness disadvantage, there is still the occluded area under the arms and between the legs in standing postures. In order to measure such area, the subject needs to make the other posture. As to time consuming disadvantage, the subject cannot strictly stay still even if the subject makes an effort to maintain the posture, the acquired shape would be little distorted. As to discreteness disadvantage, since the method of surface reconstruction of human body establishes the strict assumption, it will not work in the other postures.

In this thesis, we propose two approaches of human body modeling for tackling the incompleteness disadvantage. The first approach is that the subject will make an effort to maintain a posture which is optimal for specific measuring targets which is required in human body model in a specific application. The second approach is that the subject will variously change its posture during the measurement for fully measuring whole body without any hole since the occluded area in a posture will be measured in other postures. Under both approaches, we assume it for overcoming remaining two disadvantages that the human body consists of the rigid and almost cylindrical shaped components as follows: head, breast, waist and right and left upper arms, forearms, thighs and legs. We propose a method of segmenting the acquired shape into body components and overcoming remaining two disadvantages based on the segmentation under each approach.

Firstly, we tackle the segmentation problem under the supposition which comes from the first approach of human body modeling. The supposition is that the subject will make an effort to maintain a posture which is optimal for measuring specific targets which is required in human body model in some application. Under this supposition, we suppose that the acquired point-

cloud forms almost human body in the posture with small distortion due to little movement and some holes due to occlusion. We propose a method of segmentation based on estimating the posture of the subject from the point-cloud by matching an articulated body model. We prepare the articulated body model as the combination of cylinders, each of which represents the body component. Since the point-cloud does not contain the information of distinguishing the inside and outside of the subject in three-dimensional space, it is difficult to match the articulated body model to the point-cloud. In order to distinguish it, we construct volume model from the point-cloud and initially match the articulated body model to it. Then, we refine the estimation based on the point-cloud itself. With estimated posture, we segment the point-cloud into the body components based on distributional information of the points around each components and the information of their neighborhoods.

We tackle the time consuming disadvantage by assuming that the subject consists of multiple rigid moving objects. Although the acquired shape by light stripe triangulation would be distorted, we can correct the distortion if the object is rigid. We propose a method of acquiring undistorted shape based on segmentation and the object's motion. Since the subject consists of multiple rigid moving objects, we can correct the distortion by transforming distorted shape of each rigid component based on its motion.

We tackle the discreteness disadvantage by assuming that every body component is cylindrical shaped. Although it is difficult to reconstruct the surface for the point-cloud of the whole body which is complex shape, it is not difficult for the point-cloud of each component which has simple shape. Therefore, we perform surface reconstruction by separately reconstruct the surface for each body component.

Secondly, we tackle the segmentation problem under the supposition which comes from the other approach of human body modeling. The supposition is that the subject will variously change its posture during the measurement for fully measuring whole body without any hole based on the idea that the occluded area in a posture will be measured in other postures. Due to the subject's motion, the acquired shape would be catastrophically distorted and it does not form human body any more. Therefore, we cannot take the approach of posture estimation to segment the point-cloud. Under this situation, we assume that each component is rigid in any posture and we propose a method of segmentation which incorporates the distortion correction. We suppose that we perform distortion correction for whole point-cloud for each

body component without segmentation. Without segmentation, distortion correction would also produce superfluous shape, false shape, which does not exist in reality, since the point-cloud includes the points which belong to the other component. We perform the segmentation of the point-cloud as detecting such false shape. Since the false shape will appear in areas where the subject does not exist in reality, we calculate such area, nonexistent area, for every component based on the silhouettes of the subject for detecting the false shape. Since we can acquire segmented and undistorted shape of each component, we can acquire human body model by reconstructing the surface for each of them.

Acknowledgements

This work in Graduate School of Infomatics, Kyoto University would not have been possible if not for the support and guidance of many people.

First of all, I am especially grateful to my advisor, Professor Michihiko Minoh, for inspiring me as a visionary researcher and encouraging me as a exceptional educator. I would like to sincerely thank to the other members of my thesis committee, Professor Takashi Matsuyama and Professor Yuichi Nakamura for their constructive comments and suggestions.

I am deeply grateful to Associate Professor Koh Kakusho and Dr. Masaaki Iiyama for their terrific ideas, meticulous discussions, shrewd advice on my research. I also wish to thank Dr. Shinobu Mizuta, Mr. Isao Moro, Mr. Masahiro Toyoura, and all other members of Model group for technical discussion, and Mr. Keisuke Yagi, Associate Professor Yoshinari Kameda at Tsukuba University, Dr. Satoshi Nishiguchi, Ms. Yoko Yamakata, Dr. Tetsuo Shoji, Mr. Tomohiro Yabuuchi and all other members of Minoh laboratory for their objective comments. I also wish to express my heartfelt thanks to Mr. Tatsuhisa Yamaguchi for his voluntarily helps to construct the laser scanner. I couldn't perform several experiments without his great works. I would like to thank all of my kindful friends for encouraging me to finish my doctoral course. I also acknowledge support by research fellowships of the Japan Society for the Promotion of Science for Young Scientist. This work was partially supported by it.

Last but not least, I would like to thank my parents, Yoshikazu and Hideko, my brother, Hiroyuki, and my fiancee, Makiko for their support, patience, understanding and encouragement.

Contents

List of Figures

List of Tables

Chapter 1

Introduction

This thesis discusses human body modeling of individuals based on three-dimensional measurement. Human body model which represents the three-dimensional shape of human body is used in many fields widely. For instance, the technique of human body modeling plays an important role in anthropometry, which is the study of human body measurements for the purposes of understanding human physical variation. The CAESAR (Civilian American and European Surface Anthropometry Resource) project [25, 3] is the first three-dimensional surface anthropometry survey of about 15,000 people in three countries: U.S., Netherlands, and Italy. In the project, they measured three-dimensional shape and traditional anthropometric measurements of subjects. Anthropometry is used to optimize the design and size of ready-made products in apparel, industrial, and medical manufacturing, ergonomics, etc. Human body model of individual itself is also useful for made-to-order products design in such fields.

1.1 Conventional human body modeling

Conventionally, the posture of the subject during the measurement is assumed as standing posture in human body modeling. It is sure that the standing posture is one of the most natural postures for human, although why does it assume as the standing posture? Some reasons for the assumption come from the principle of the measurement method.

Many methods have been proposed for measuring three-dimensional shape of object as follows: stereo [21], photometric stereo [34], shape from silhou-

ette [16], etc. Each method has advantages and disadvantages, and we need to take it into consideration for choosing a method that the features of subject and requirements of the measurement. Since the human body is less textured and the model should be accurate, light stripe triangulation is the best principle of the measurement. For instance, many commercial products [9, 11, 12, 10] which have been developed for measuring three-dimensional shape of individual body is based on light stripe triangulation, which has an accuracy of about 0.5mm.

In light stripe triangulation, we project the laser sheet onto the subject and observe the illuminated part by calibrated camera(s). We can calculate the three-dimensional shape of the illuminated part based on the triangulation. For a moment, we can only acquire the shape of the part where is illuminated by the laser sheet, which is as a thin stripe on the subject's surface. In order to acquire the full shape of the subject, the laser scans the whole subject and the cameras observe the scanning. Light stripe triangulation can accurately measure the three-dimensional shape of an object, although the method has three disadvantages in human body measurement.

1. Incompleteness.
2. Time consuming.
3. Discreteness.

The first disadvantage is '*incompleteness*'. As stated above, we can acquire only the part where is illuminated by the laser sheet and visible to the camera directly. A human body has a complex shape that some parts are occluded from laser sheet or limited cameras in any posture, and we cannot measure the shape of such occluded part. Hence, we cannot acquire complete human body model in single posture. It is desired for a posture during the measurement that the occluded part of the subject is minimized as possible.

The second disadvantage is '*time consuming*'. It takes a certain time to scan the whole subject with a laser sheet. In the case of whole body measurement, it takes about dozen of seconds. If the subject moves during the scanning, the measurement results become distorted and the accuracy is degraded. Basically it is necessary that the subject stays still while scanning for avoiding distortion in the results. Hence, it was desired for a posture during the measurement that the subject can maintain the posture as still.

The third disadvantage is '*discreteness*'. The shape of the subject is acquired by light stripe triangulation as dense points, which is termed as

point-cloud, on the surface. Such point-cloud is not a continuous surface which explicitly represents the shape, but just scattered points which implicitly represent the shape. For acquiring the shape of the subject, we need to reconstruct a surface from the point-cloud. Several methods [2, 5, 18, 17] have been proposed for reconstructing a surface from point-cloud of a general object, but they assume that the point-cloud is uniformly distributed without holes on the subject's surface. Such methods are not suitable for point-cloud of a human body with holes in the occluded areas, since these methods would produce obstructive surface which cover concave area such as the armpits and crotch.

Conventionally, it is supposed that the subject will maintain the standing posture during the measurement. Under this supposition, it is assumed for overcoming the disadvantages in light stripe triangulation that the shape of subject is roughly known, and the subject is treated as a stationary rigid object during the measurement. Firstly, most parts of the body are easily visible to the laser and cameras in the natural standing posture except for the areas under the arms and between the legs. For reducing the occluded areas, the standing posture with holding arms and legs away from the body is desirable during the measurement. Secondly, the standing posture is one of the most stable in all postures which satisfy previous condition. With several methods [20, 31, 27, 6] which speeding-up the measurement, the subject will be able to maintain the standing posture as still during the measurement, so the distortion in measurement results will be reduced. Thirdly, Douros et al. have been proposed a method [4] for reconstructing a surface from point-cloud of a whole human body in standing posture. Although the method establishes a number of strict assumptions, including the roughly shape of the subject, they are satisfiable in the conventional human body measurement.

1.2 Human body modeling in various postures

The acquired human body model represents the shape of human body in the posture during the measurement. With conventional system, we can acquire the human body model only in standing posture. Although such human model will be fundamental material for the study of understanding human physical variation, it is not always adequate for made-to-order products de-

sign in many fields. Each of products design will require different part of human body model; the design of glove will require the hand, and the design of stocking will require the lower body, etc. The standing posture is not always optimal for measuring a specific part; the areas under the arms and between the legs are still easily occluded in the standing posture, so such areas of human body would not be measured. Strictly speaking, the posture during the measurement shall be determined based on the targets in the human body which comes from the usage of the model for overcoming 'incompleteness' disadvantage of light stripe triangulation.

In this thesis, we present two concrete approaches for overcoming 'incompleteness' as follows:

1. Measuring a posing subject in the posture which is optimal for measuring specific targets in the human body.

2. Measuring a moving subject for making many postures in order to make complete human body model.

In order to overcome remaining two disadvantages, we assume that the human body in arbitrary postures consists of the rigid and almost cylindrical shaped components as follows (see also Figure 1.1): head, breast, waist and right and left upper arms, forearms, thighs and legs.

1.2.1 Human body modeling of posing subject

The first approach supposes that the subject will make an effort to maintain the posture which is optimal for measuring specific targets in the human body. When we suppose that the subject will not maintain the standing posture, but be in a posture during the measurement, we must overcome remaining two disadvantages of light stripe triangulation, which are 'time consuming' and 'discreteness', without the assumption that the subject will maintain the standing posture.

The 'time consuming' disadvantage would make the distortion in acquired point-cloud when the subject would move. In the conventional human body modeling, it is assumed that the distortion in point-cloud will be negligible since the subject stays still by maintaining the standing posture, which is stable posture. However, when the subject makes an unbalanced posture for reducing the occlusion in the specific targets, the subject cannot stay still as stationary object and the distortion in point-cloud will not be negligible. For

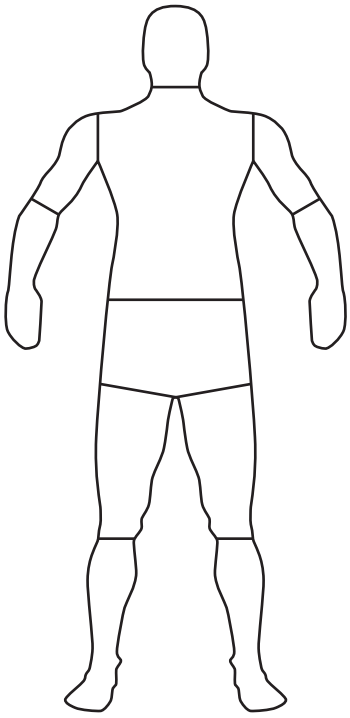

Figure 1.1: Human body components.

overcoming this problem, we propose a method of correcting the distortion in point-cloud by assuming that every component of human body is rigid. The proposed method also measures the motion of the body components during the light stripe triangulation, and corrects the distortion in point-cloud based on the motion for each component. However, it is necessary for performing the correction to segment the point-cloud into the components of the human body since the distortion correction should be performed for each component.

The 'discreteness' disadvantage causes a problem of surface reconstruction. When the subject is not in standing posture, the method of Douros et al. [4] would not work since its strict assumptions would not be satisfied. For overcoming this problem, we propose a method of reconstructing the surface in each component separately with simple procedure by assuming that every component of human body has simple cylindrical shape. As the same in distortion correction, it is also necessary to segment the point-cloud into the components since the surface reconstruction should be performed for each component.

Since the methods of overcoming two disadvantages are based on the segmentation, we propose a method of segmenting the point-cloud into body components under the approach to overcome the 'incompleteness' disadvantage. Under the approach, we assume that the motion of each component of the body will be relatively small since the subject will make an effort to make the posture. Although the measuring results would be little distorted, it will form almost human body. This assumption affords a clue to solve the segmentation problem. Here, we introduce an articulated body model and estimate the posture of the subject from point-cloud by using it. The articulated body model consists of a number of elliptical cylinders, each of which represents rough shape of the component of the human body and is connected with a joint. After estimating the posture, we segment the point-cloud into the rigid components based on the articulated body model. The distortion correction and the surface reconstruction are performed based on this segmentation result for acquiring the human body model of the subject in the posture. We discuss the detail of this approach in Chapter 3. We describe the proposed process of human body modeling in Figure 1.2.

1.2.2 Human body modeling of moving subject

The second approach supposes it for overcoming the 'incompleteness' disadvantage that the subject will make many postures during the measurement

for fully measuring whole body. This approach is based on the idea that the area which cannot be measured due to occlusion in a posture will be measured in other postures. We will be able to make complete human body model by integrating the measurement in many postures.

As mentioned above, we attempt to overcome remaining two disadvantages of light stripe triangulation based on the segmentation. However, we need to tackle the segmentation problem in another way since the supposition is different to the previous approach. Under the second approach, we suppose that the subject will variously change its posture during the measurement for fully measuring whole body without any hole since the occluded area in a posture will be measured in other postures. Due to the subject's motion, the acquired shape would be catastrophically distorted and it does not form human body any more. Therefore, we cannot take the approach of posture estimation to segment the point-cloud. Under this situation, we assume that each component is rigid in any posture and we propose a method of segmentation by finding the part which is not change its shape in many postures based on the motion of each component. In this approach, it is not necessary that each measurement in a posture is not approximately complete; it is only necessary that every area is measured at least once in some postures. Hence, there is no need to acquire undistorted whole human body model in each posture, so the subject can move freely during the measurement. We discuss the detail of this approach in Chapter 4.

These two approaches have both merits and demerits in several aspects about descriptive power of the modeling. Firstly, in completeness aspect, the first approach will produce model which is complete only in specific targets, but the second approach will produce fully complete model. Secondly, in posture variation aspect, the first approach will produce model only in a particular posture, but the second approach will produce models in many postures. Under the assumption in the second approach, whole body will be same shape as the combination of the components of the body. So, the shape of whole body in arbitrary posture can be produced by rearranging the components to its position in the posture. Thirdly, in the degree of detail aspect, the first approach will produce more detail model than the second approach. In order to overcome 'time consuming' disadvantages, we establish the same assumption that every component of human body is rigid under both approaches. Strictly speaking, however, the components of human body will change its shape a little with various postures due to muscle contractions. Although the shape will not change much locally when the subject

make an effort to maintain the posture as in the first approach, it will little change when the subject changes its posture variously. Therefore, the first approach can describe detail shape in the particular posture, however the second approach ignore the changing of the shape in each component.

1.3 Overview of thesis

This thesis consists of five chapters.

In Chapter 1, we have discussed human body modeling as the introduction.

In Chapter 2, we show the principle of light stripe triangulation and its disadvantages. We also discuss the conventional approach to the human body modeling.

We present our two approaches to human body modeling in Chapter 3 and 4, respectively.

In Chapter 5, we conclude the thesis with some discussion and future works.

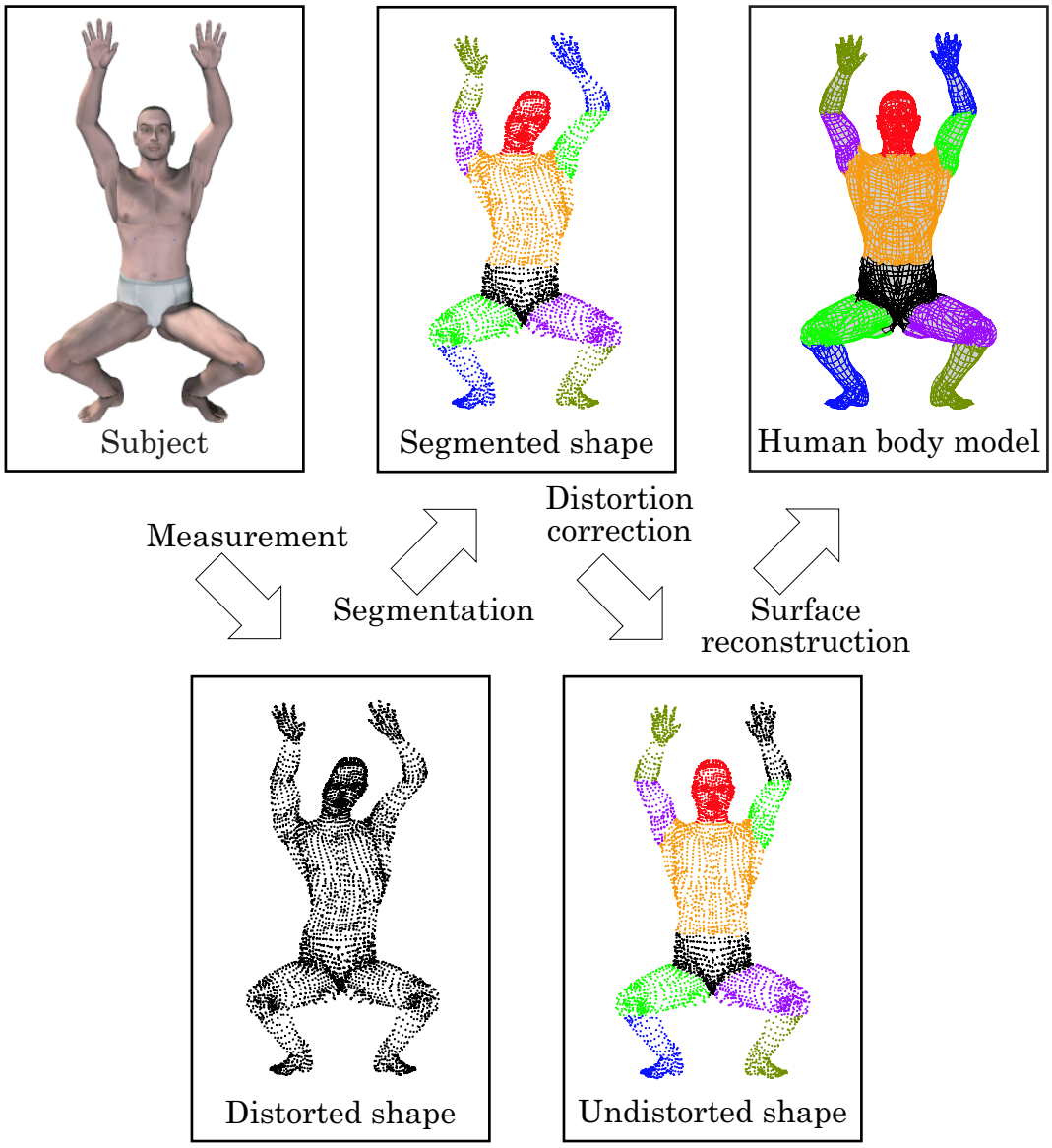

Figure 1.2: Process of human body modeling.

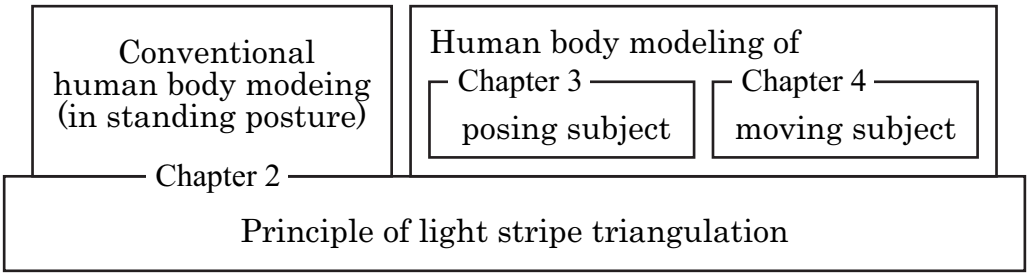

Figure 1.3: Scheme of this thesis.

Chapter 2

Conventional human body modeling

In this chapter, we discuss the principle of light stripe triangulation and its disadvantages. Then, we discuss the tackling of conventional human body modeling for the disadvantages.

2.1 Principle of light stripe triangulation

Light stripe triangulation is a well-known non-contact method for measuring three-dimensional shape of an object. This method is performed as follows:

1. Project a laser sheet onto the subject.
2. Observe the projected laser sheet, which is observed as a thin stripe on the subject's surface, with calibrated camera(s).
3. Calculate the 3D position of the points that are on the observed stripes in the camera image from the position of the plane of the laser sheet and the pose of the camera by using the triangulation (see also Figure 2.1.).

From camera image at a moment, we can acquire only the partial shape of the whole subject where is illuminated by the laser sheet as a number of points. In order to acquire the full shape of the subject, the laser scans the whole subject and the cameras observe the scanning (see also Figure 2.2.) In comparison with other 3D shape capture methods, this method can acquire

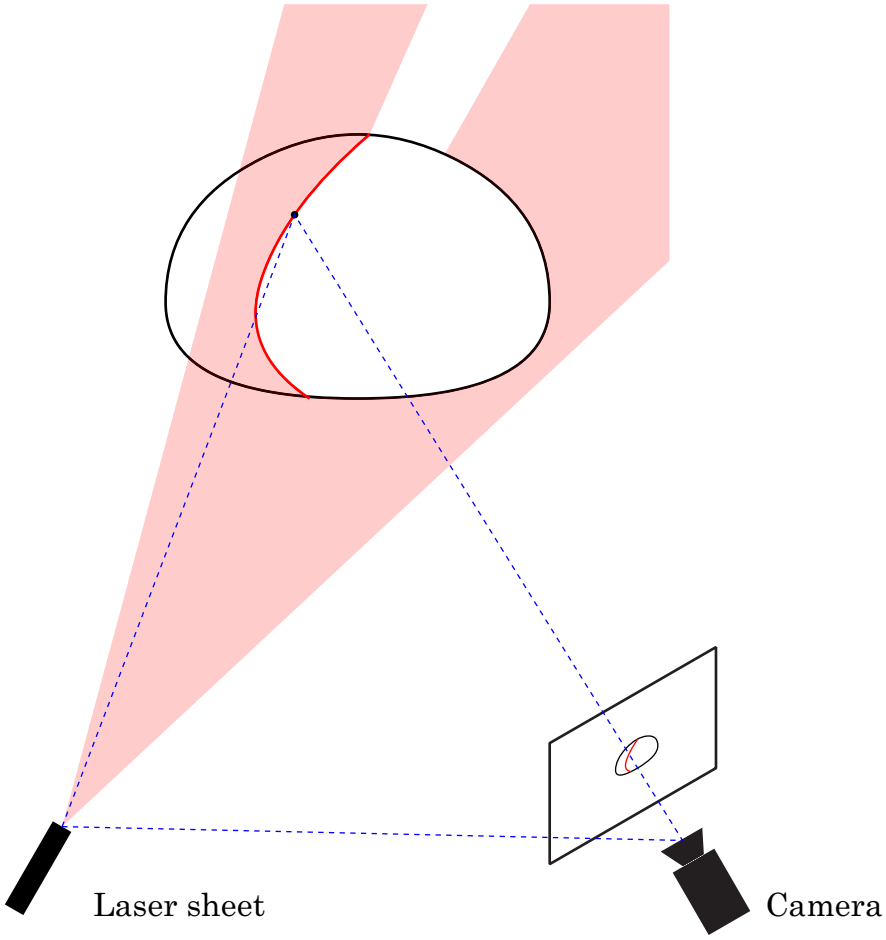

Figure 2.1: Principle of light stripe triangulation.

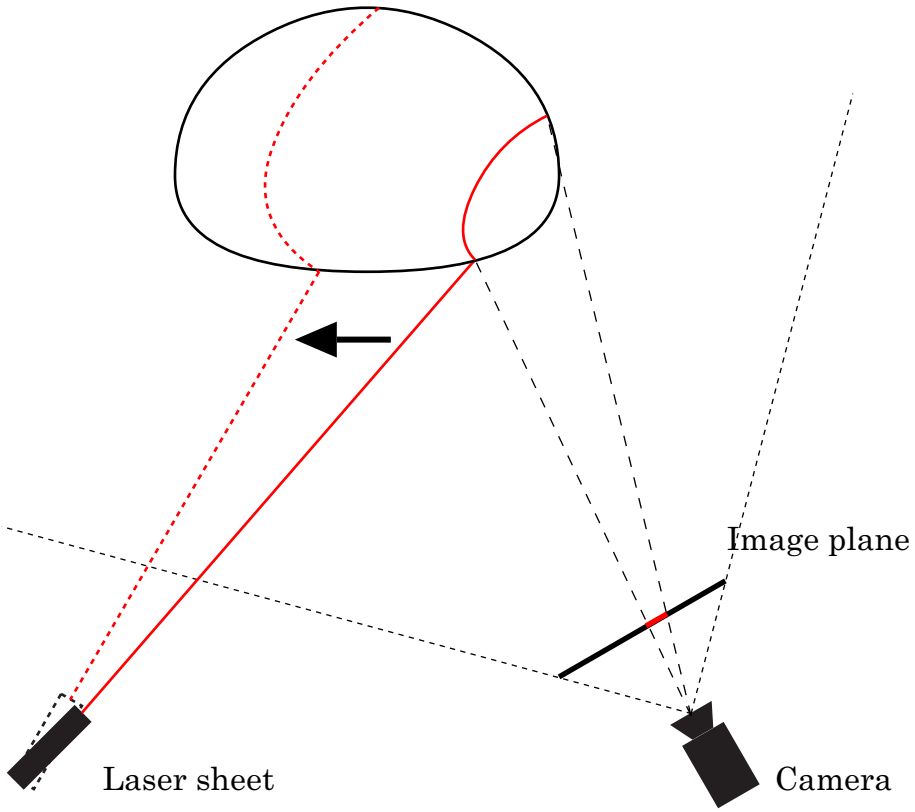

Figure 2.2: Laser scanning.

high resolutional and accurate shape but has several disadvantages due to its principle. In this thesis, we discuss three disadvantages as follows:

1. Incompleteness
2. Time consuming
3. Discreteness

2.1.1 Incompleteness disadvantage

The first disadvantage is '*incompleteness*'. As mentioned above, light stripe triangulation can measure the shape where is illuminated by the laser sheet and is directly visible to cameras. In order to performing the triangulation, it

is necessary to be known that the position of the plane of the laser sheet and the pose of the cameras. Sometimes, the camera and the laser sheet are fixed and the laser scanning is performed as optical reflection by using the mirror which has an electrically controlled mechanism of the rotational oscillation (galvanometer mirror). When we observe the laser scanning with cameras, some areas of the subject would be occluded from such limited sensors. We cannot acquire the shape in such area.

2.1.2 Time consuming disadvantage

The second disadvantage is '*time consuming*'. From camera image at a moment, we can acquire only the partial shape where is illuminated by the laser sheet. It takes much time for scanning the whole subject with the laser sheet. In order to densely acquire shape of the subject as a number of stripes, we need to acquire many camera images of the laser scanning. With usual camera, which can capture at most few dozens of images per a second, it consumes time to densely acquire the subject's shape. This disadvantage causes a problem when the subject moves during the scanning. When the subject stays still during the scanning, we can acquire an accurate shape of the subject as depicted in Figure 2.3 (a). However, when the subject would move during the scanning, the acquired shape would be distorted by the subject's motion during the scanning as depicted in Figure 2.3 (b).

2.1.3 Discreteness disadvantage

The third disadvantage is '*discreteness*'. As mentioned above, the shape of the subject is acquired as a number of points which are placed on the subject's surface in three-dimensional space. In this thesis, we call these points as *point-cloud*. Point-cloud is discrete, not continuous, description of the shape, since it is acquired from the camera images which are spatio-temporally discrete. Point-cloud only represents the position of points where the subject's surface is, however, not the surface itself explicitly. In order to acquire explicit representation of the surface from point-cloud, we need to construct the surface by making connectivity among point-cloud. This problem is well-known as surface reconstruction.

Several methods have been proposed for reconstructing surface from point-cloud of general object. Amenta et al. [2] and Fang et al. [5] present methods based on Delaunay triangulation in three dimensions. Metaxas et al.

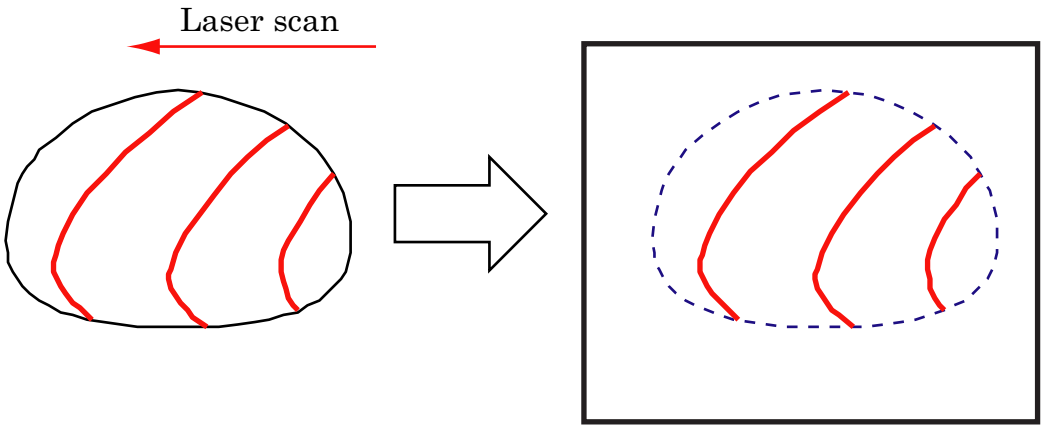

(a) Light stripe triangulation for stationary object

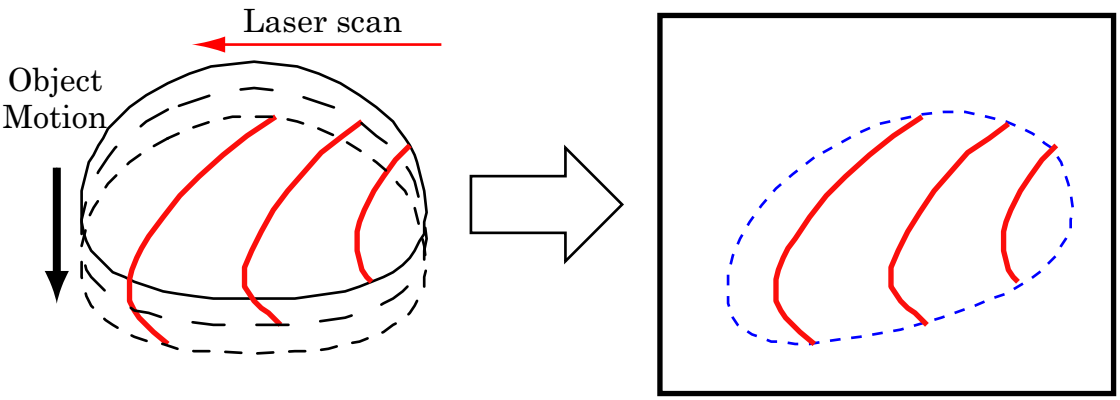

(b) Light stripe triangulation for moving object

Figure 2.3: Distortion problem.

[18] present a method which estimates the object's surface based on the deformable superquadric model. These methods assume that the point-cloud is dense and uniform. Matsuoka et al. [17] present a method which constructs basic mesh as a surface of volume model. That volume model is constructed from point-cloud. Then, the dense mesh is constructed for point-cloud based on the basic mesh. In this method, the size of voxel which constructs volume model is determined by the density of the point-cloud.

2.2 Conventional human body modeling and its problems

Conventionally, it is supposed for tackling the 'incompleteness' disadvantage that the subject stays still by maintaining standing posture during the measurement. Under this supposition, several method have been proposed for tackling the remaining disadvantages of light stripe triangulation.

2.2.1 Tackling for the incompleteness disadvantage

In the natural standing posture, most parts of the body are easily visible to the laser and cameras except for the areas under the arms and between the legs. For reducing the occluded areas, the standing posture with holding arms and legs away from the body is desirable during the measurement.

However, we can only acquire the human body model in standing posture with this approach. Although such human model will be fundamental material for the study of understanding human physical variation, it is not always adequate for made-to-order products design in many fields. Each of products design will require different part of human body model; the design of glove will require the hand, and the design of stocking will require the lower body, etc. The standing posture is not always optimal for measuring a specific part; the areas under the arms and between the legs are still easily occluded in the standing posture, so such areas of human body would not be measured. Strictly speaking, the posture during the measurement shall be determined based on the targets in the human body which comes from the usage of the model for overcoming 'incompleteness' disadvantage of light stripe triangulation.

2.2.2 Tackling for the time consuming disadvantage

The distortion problem will often occur when scanning the human body. Some commercial products [9, 11, 12, 10] take about a dozen of seconds to scan the whole body with accuracy of about 0.5mm. In order to acquire the distortion-free shape, the subject needs to stay still during the scanning for a dozen of seconds. Although the subject makes an effort to maintain the posture, the subject periodically moves slightly for making balance.

This periodic motion in standing posture, which is called as *trunk sway*, is observed to assess postural stability in medical, physiological and biomechanical science. In [32, 33, 29, 26, 8], the trunk sway is observed as the movement of body center-of-mass (COM) and is regarded as the oscillation of an inverted pendulum. As has been reported in [32], the average absolute amplitude and the average frequency of the oscillation are about 5mm and 1Hz, respectively. Furthermore, the amplitude of the trunk sway would be increased in unstable postures. Such oscillation will seriously distort the shape acquired with accuracy of about 0.5mm by light stripe triangulation.

As a tackling with the problem, several methods of speeding up the measurement are applicable. Speedy scanning will make the distortion small.

Distortion reduction by speeding-up the measurement

Under the same condition of the subject's motion, the degree of distortion depends on the amount of measurement time. So, speeding up the measurement will reduce the distortion in acquired shape by light stripe triangulation. However, speeding up the laser scanning decreases the resolution of measurement under the same frame rate of the camera. In order to maintain the resolution of the measurement, it is necessary to increase both the frame rate of the camera and the power of the laser[20]. It is not undesirable that the scanning with high power laser for safety reasons.

Parallelizing the scanning with multiple lasers will also allow us to speed up the measurement without speeding up the scanning itself. For example, the measurement in same resolution by using 3 lasers, which is as depicted in Figure 2.4, will takes 1/3 of the time which takes in scanning by using single laser. We can consider that if we use a lot of lasers, it will take less time in scanning, and we will be able to acquire almost distortion-free shape. However, using a lot of lasers causes problems for triangulation.

One problem is making correspondence. As mentioned above, it is re-

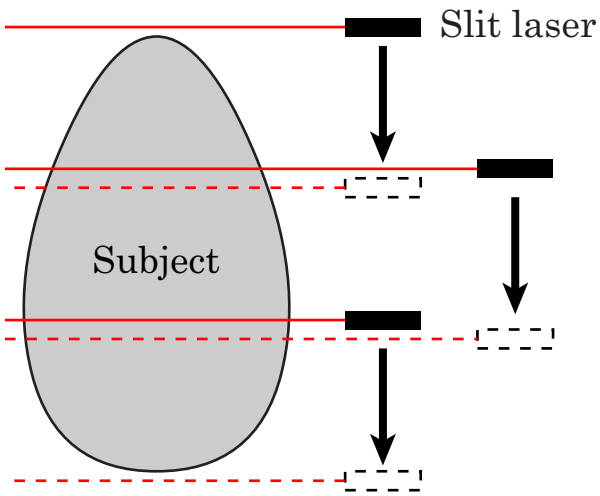

Figure 2.4: Parallelized scanning decrease scanning time.

quires for triangulation that the position of the plane of the laser sheet which is observed in camera image. In order to performing triangulation, we need to make correspondence between the observed stripe in camera image and the laser sheets when we use a lot of lasers. As depicted in Figure 2.5, miscorrespondence causes that calculated position of the point is different from the real position, and we cannot acquire correct shape of the subject. Several methods [31, 27, 6] have been proposed for parallelizing the scanning and making the correspondence by using multiple color lasers or light patterns projection (see also Figure 2.6).

Although these methods are applicable to a stationary object, another problem will occur when they are applied to a moving object. Figure 2.7 illustrates vertical scanning of an object which moves horizontally. With a single laser (see Figure 2.7-a), the acquired shape is distorted due to the object's motion. In comparison with single scanning, parallelized scanning can acquire less distorted shape (see Figure 2.7-b). However, the acquired shape is segmented, and each segment (A, B in Figure 2.7-b) will not match because the time of capture is different between borders (the bottom of A and the top of B). This problem is inevitable when parallelized scanning is performed to moving subject in a certain time, not a moment.

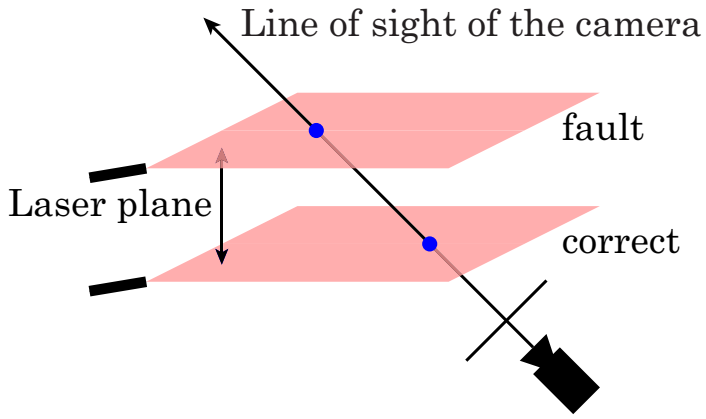

Figure 2.5: Correspondence problem in multiple scanning.

Figure 2.6: Light patterns used for projection.

2.2.3 Tackling for the discreteness disadvantage

There will be holes in the point-cloud due to 'incomplete' disadvantage of light stripe triangulation. This means that we cannot apply several conventional methods [2, 5, 18, 17] for surface reconstruction since the point-cloud is not uniform.

The point-cloud which is acquired from human body also represents complex shape. For example, there are several concave areas around the armpits and crotch in standing posture. In any posture, there will be concave areas in human body surface since human body has articulated structure with a lot of components. The conventional methods have a problem that reconstructed surface will cover with the concave areas such as the armpits and crotch in standing posture as depicted in Figure 2.8. This problem will occur since the nearest points are simply connected.

In order to avoid the invalid surface, Douros et al. have been proposed a method [4] for reconstructing a surface from point-cloud of human body. They segment the point-cloud of human body in standing posture into several parts as depicted in Figure 2.9. When the segmentation is correctly

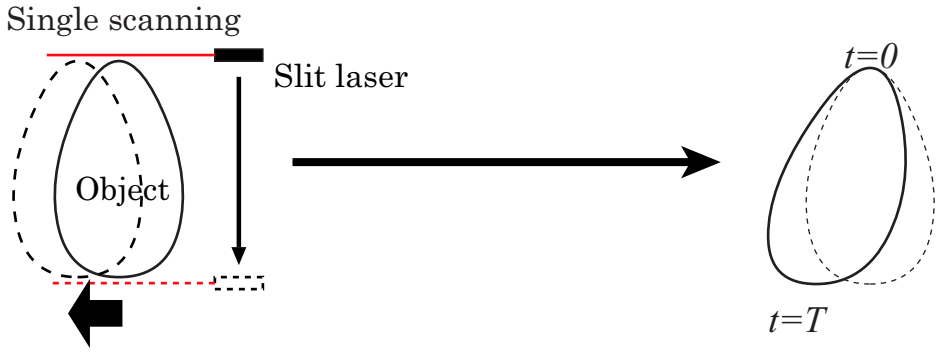

(a) Scanning with single laser.

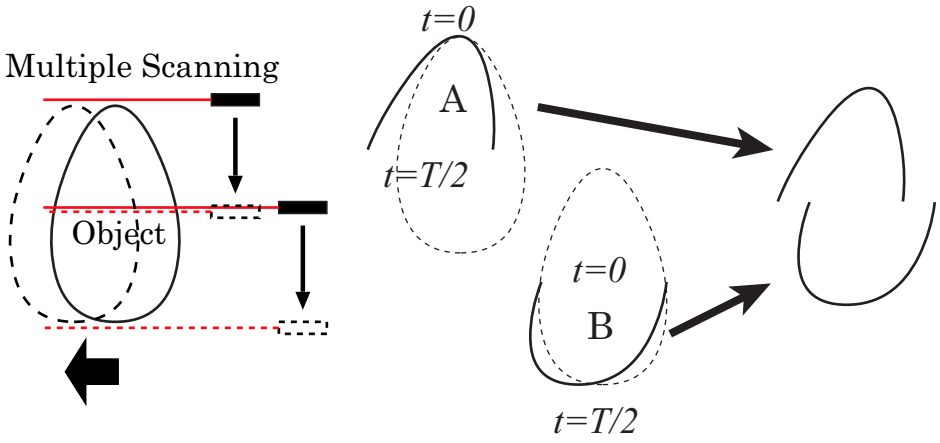

(b) Scanning with multiple lasers.

Figure 2.7: Mismatch problem in parallelized scanning.

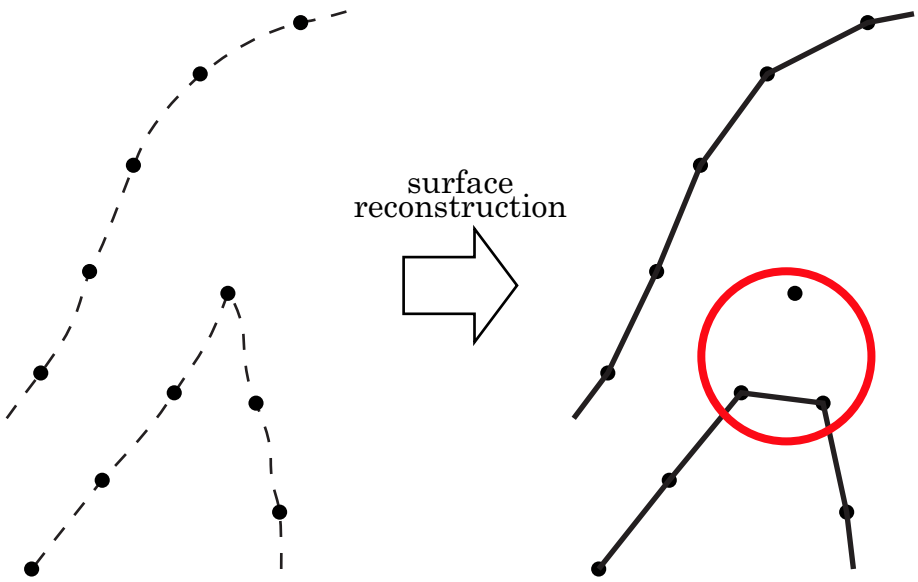

Figure 2.8: Reconstructed surface cover the concave area.

performed, it is assumable that any horizontal slice in part (a) will form two ellipses. Similarly, there is one, three, and one slices in part (b), (c), and (d), respectively. Based on this assumption, it is possible to reconstruct surface for the point-cloud without invalid surfaces.

In order to perform the segmentation, they establish a number of assumptions, especially strict for the posture. Ju et al. [14] also have been proposed similar automatic segmentation. Therefore, these method is not applicable to the measurement in the other postures due to its strict assumptions.

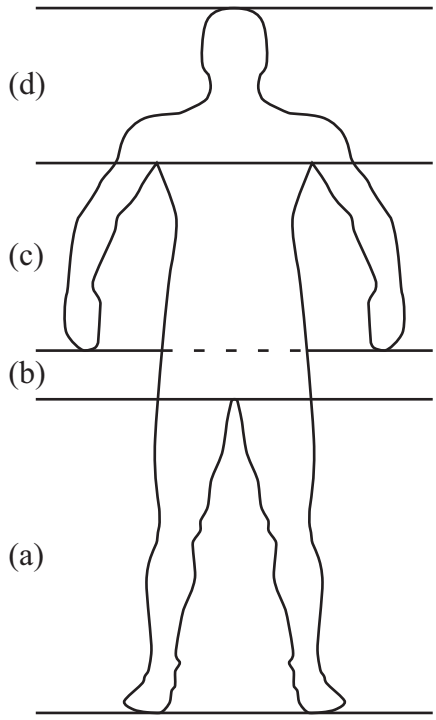

Figure 2.9: Body structure in standing posture.

Chapter 3

Human body modeling of posing subject

3.1 Introduction

In this chapter, we suppose that the measurement is performed with the first approach for overcoming 'incompleteness' mentioned in Section 1.2.1, and propose a method of human body modeling. The approach supposes that the subject will make an effort to maintain the posture which is optimal for measuring specific targets in the human body. Under the approach, we must overcome remaining two disadvantages of light stripe triangulation, which are 'time consuming' and 'discreteness'.

In order to overcome 'time consuming' disadvantage, we assume that human body consists of rigid components and propose a method of correcting the distortion in acquired shape based on the motion of each component during the measurement as substitute for speeding up the measurement. It is necessary for performing the distortion correction that we segment the point-cloud of whole body into each body components and measure the motion of every body component.

In order to overcome 'discreteness' disadvantage, we assume that every body component is almost cylindrical shapes. Under this assumption, we can reconstruct surface for each component easily. By segmenting the point-cloud into body component, we can acquire whole surface without invalid surfaces by reconstructing surface separately for each component and combining them.

We need to segment the point-cloud into body components for overcoming both of disadvantages. In order to perform segmentation, we make several suppositions for the acquired point-cloud under the approach as follows:

- The point-cloud forms almost human body, although it would be distorted a little by the movement to keep the balance for maintaining the posture.
- The subject does not always make standing posture. It depends on the measuring targets.
- The point-cloud will be incomplete in some area due to self-occlusion, but forms whole body.

Under these supposition, we propose a method of segmentation based on the posture estimation of the point-cloud. We also suppose that the size of the subject's body is roughly known, and prepare an articulated body model based on it. The articulated body model consists of the components of human body and it can roughly represent the human body shape in any posture. We estimate the posture of the point-cloud by using the articulated body model, and segment of the point-cloud into the body component based on the articulated body model.

3.2 Point-cloud segmentation based on posture estimation

3.2.1 Posture estimation from point-cloud

In order to estimate the posture of the point-cloud, we match the articulated body model with the point-cloud. The point-cloud only represents that there is the surface of the subject, but does not contain the information of distinguishing the inside and outside of the subject in three-dimensional space. Therefore, it is difficult to match the articulated body model to the point-cloud without the information. In order to distinguish the inside and outside of the body in three-dimensional space, we construct volume model from the point-cloud. Then, we roughly estimate the posture by matching the articulated body model to the obtained volume model, and refine the estimation by matching the articulated body model to the point-cloud directly.

Figure 3.1: Articulated body model.

Articulated body model

The articulated body model consists of the body components, which are supposed as the head, chest and waist, and the right and left upper arms, forearms, thighs, and legs. We represent cylindrical part of each component as the three-dimensional elements, which is cylinder or elliptic cylinder, and join them for constructing the whole body as depicted in Figure 3.1. The cylinders and elliptic cylinders are connected at joint and they can rotate around the joint. In order to determine the initial position in the posture estimation, we create a cylinder which covers the chest and waist as the torso. We set the size of each element in accordance with rough size of the subject's body and anthropometric statistics.

We define the center of gravity for the articulated body model in accordance with the center of gravity of the point-cloud for initial positional estimation of the point-cloud. Preliminary experiments have shown that the center of gravity of the point-cloud is almost always in the lower waist, regardless of the absence of points or of the posture of the subject. We define the center of gravity of the articulated body model as the midpoint of the axis of the elliptic cylinder which representing the waist of the human body.

Constructing volume model from point-cloud

We construct the volume model by applying the method of Matsuoka et al. [17]. They determined the voxel size by calculating the density of the sparsest part of the point-cloud. They defined the contour voxels for the point-cloud by using the voxel size, and constructed the volume model as the part surrounded by the contour voxels. In our case, however, the voxel size is greatly enlarged if the point-cloud contains holes in occluded area. Thus, it is impossible to represent spacing, such as that between the chest and the upper arm, which makes it difficult to estimate the posture by matching of the articulated body model.

We introduce upper and lower limits for the voxel size so that the constructed volume model will be consistent with the human shape. Figure 3.2 shows the constructed volume model. When the voxel size is limited, it is sometimes impossible to construct contour voxels which cover the whole surface of the object. It makes impossible to determine the inside voxels precisely. Furthermore, neither the contour voxels nor the inside voxels will not be constructed for parts where there are big holes. However, since the purpose is to construct volume model which provide clues for posture estimation, there is no problem if we cannot construct complete volume model.

Initial estimation from volume model

We perform matching the articulated body model to the volume model which is constructed as described above. The matching is performed successively from the chest, with a large volume, to the extremities as depicted in Figure 3.3.

Firstly, in order to match the initial position of the articulated body model to the point-cloud, whole articulated body model is aligned so that the center of gravity of the articulated body model is fit to the center of gravity of the point-cloud. Then the torso, which has the largest volume in the articulated body model, is matched to the volume model. After that, matching of the body component is performed from the chest to the extremities, in the order of the chest, the right and left upper arms and forearms, and the thighs and legs.

Matching is performed as that the body component of the model is moved with translation and rotation, to obtain the best agreement of the model with

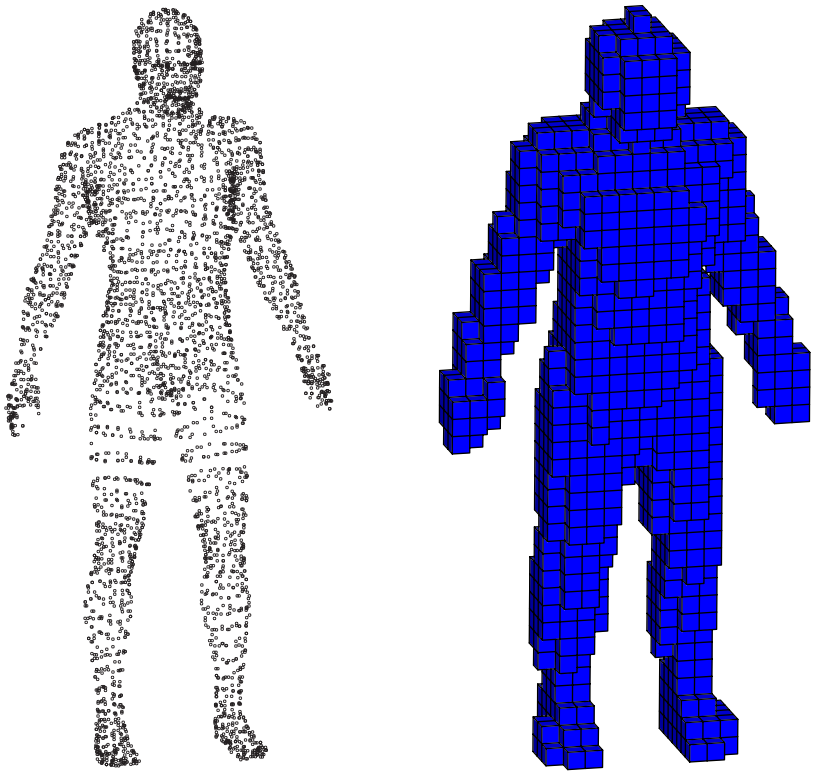

Figure 3.2: Volume model (right) from point-cloud (left).

the volume model. In the matching of the torso, a weight is assigned to the contour voxel, so that the body component is matched as closely to the center of the volume model as possible.

Improving estimation accuracy based on point-cloud

Based on the results of initial matching with the volume model, we extract the points which are located within a certain distance from the surface of each body component of the articulated body model as the '*surface point*' of the body component. Then, the positions and angles of the body components (posture) are adjusted so that the square-sum of the distances from the model surface of body component to the points is minimized. Since the width and length of each body component of the articulated body model are determined from statistical data, they may deviate from the actual size of the body component of the subject. Therefore, we adjust the radius and length of the cylinders composing the articulated body model based on the point-cloud. The radius is set as the average distance from the central axis of the model to the surface point. The length is determined by estimating the ends of the body component. The end of the body component is estimated by locating the surface point for which the distance from the central axis of the model falls below a preset threshold. If such a point cannot be found, it is supposed that the end of the body component is not closed, and the length is not adjusted. For example, the end of the body component cannot be identified in a posture with an extended arm. However, it does not cause problem in both distortion correction and surface reconstruction. In the distortion correction, it can be supposed that there will be little difference between the transformations of two connected body components around their joint since we suppose that the subject will maintain its posture. Therefore, the points around the joint will correctly transformed if the point is segmented into either two of connected body components. In the surface reconstruction, it is not problem since the point-cloud around the joint will not generate invalid surface.

3.2.2 Point-cloud segmentation based on body model

We present a method of segmenting the point-cloud into the body component by using the articulated body model with the estimated posture. Let us consider that we perform the simple segmentation of the points by just

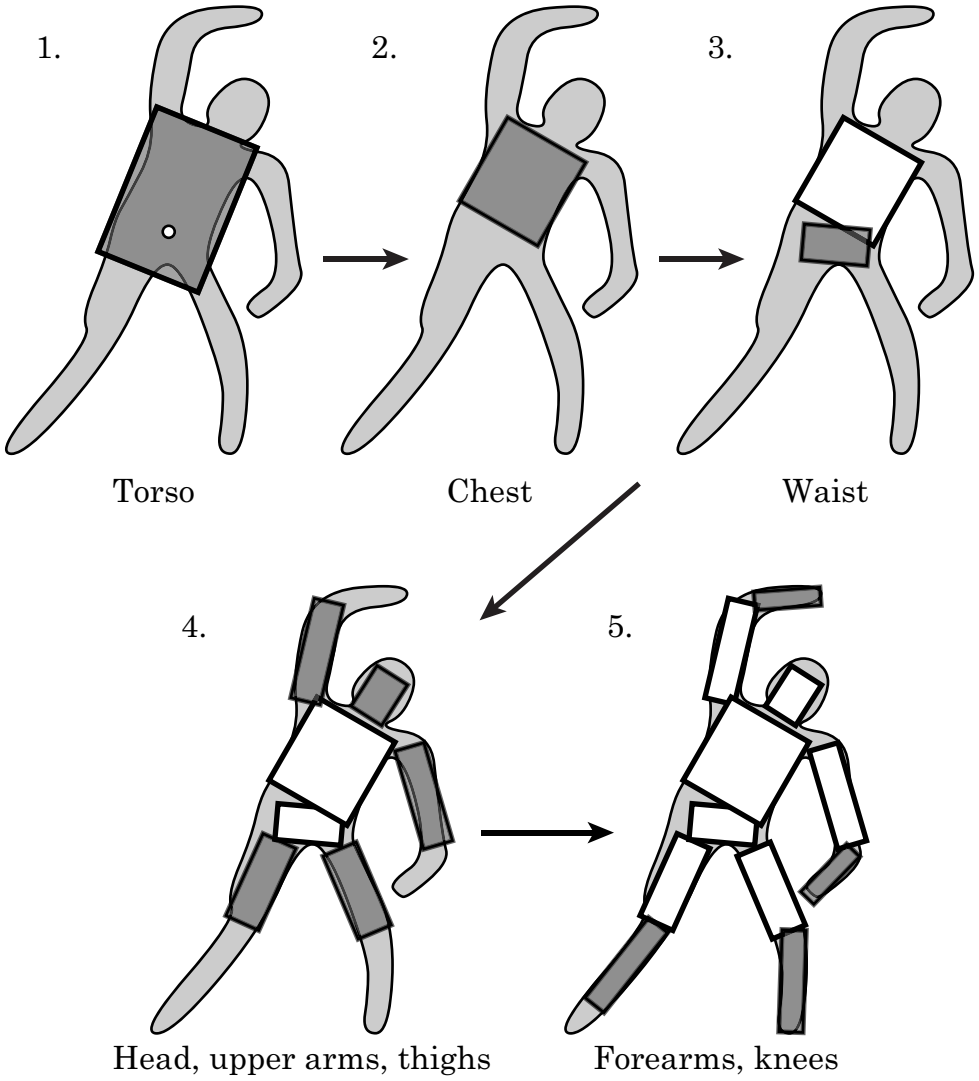

Figure 3.3: Model matching with volume model.

making the threshold T_d for the distance from each point to the model surface of body component of the articulated body model. As a result, the points at parts such as the armpits in standing posture, where multiple body components are close to each other but not connected in practice, will be segmented into multiple body components, and this causes problems in the distortion correction and the surface reconstruction.

In the proposed method, we refine the segmentation by using the distribution of the distance from each point to the model surface of component for correcting the results of simple segmentation based on the threshold T_d. Even if we perform this processing, some points which are segmented into multiple body components will still remain. Except for around the joints, we choose a single component, which we denote as segmenting destination, for such points by utilizing the segmentation result of neighborhoods as far as possible.

Segmentation based on distance distribution

In order to represent the position of each point in the point-cloud, we adopt the cylindrical coordinate system for each component of the articulated body model. We denote the component along the axis of the cylinder composing the body component as h, the distance from the cylinder surface as r, and the angle on the plane perpendicular to the axis of the cylinder as θ ($0 \leq \theta \leq 2\pi$). The direction of the angle 0 is set arbitrarily.

Since the body component is not a cylinder or elliptic cylinder in practice, there are fluctuations in the distance from the model surface of component to the actual surface of the subject. In addition, when a surface belonging to multiple different body components exists in the neighborhood, as in the cases of the armpit and crotch in the standing posture, the distance r to the model surface of the component does not differ much between the surface of the component and the surface of another component. For example, the relatively thin part of the waist, and assume that the surface of another body component, that is, the forearm, exists in the neighborhood as depicted in $h3$ of Figure 3.4(a). Then, the distance to the surface of the forearm does not differ much from the distance to the surface of the relatively thick part of the waist as depicted in $h1$ of Figure 3.4(a). In such case, the distributions of the distance r from the point-cloud belonging to the respective body component to the surface of the waist model will overlap. It is difficult to exclusively extract all points of the waist from the whole point-cloud, regardless of what

threshold T_d is set for r.

Since the surface has the properties of continuity and smoothness in practice, the distance from the model surface of a component to the surface of the corresponding body component of the subject does not change much locally. In regard to the local distributions of the distance from the model surface of component, there is difference between the surface of corresponding body component and the surface of other body components, except for the joints. Therefore, the local distributions of distance from the model surface to the point-cloud which is acquired from different body component surfaces do not overlap, and it is possible to segment them by means of a threshold as depicted in Figure 3.4(b). We investigate the distribution of distance r of the points which exist nearby the model surface of component in local area, which is mesh of the side face of the cylinder in the model component which is divided according to the values of (θ, h) as described in Figure 3.4(c).

In this method, we acquire the threshold that segment the point-cloud into body components for each local area of the body component by applying discriminant analysis to the local distribution of distance r. We suppose that simple segmentation is applied beforehand using the threshold T_d, and that the point-cloud is extracted for each body component, with points belonging to at most two body components locally. When the distribution of the point-cloud with respect to r is composed of two single-peaked distributions, an appropriate threshold can be determined by constructing a histogram of the r component and applying discriminant analysis [22].

Meanwhile, the distribution should not be divided if the point-cloud forms a unique single-peaked distribution, since the point-cloud in that local area will be only from the body component. In this method, when the number of points having values of r close to the threshold obtained by discriminant analysis is larger than some threshold T_n, it is determined that the distribution has a single-peaked and all points belong to the body component. When the point-cloud in a mesh has two single-peaked distributions, it is determined that the distribution with the smaller r is from the body component, and that the distribution with the larger r is representing the surface of another body component. Then, the points with an r component smaller than the obtained threshold are segmented into the body component.

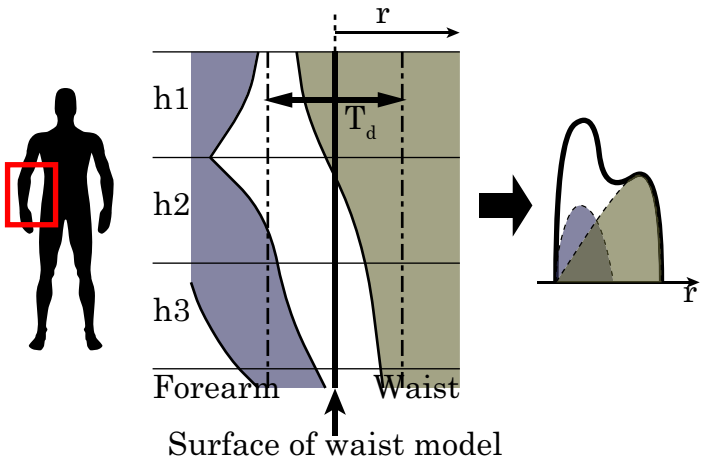

(a) Distribution of point-cloud on components

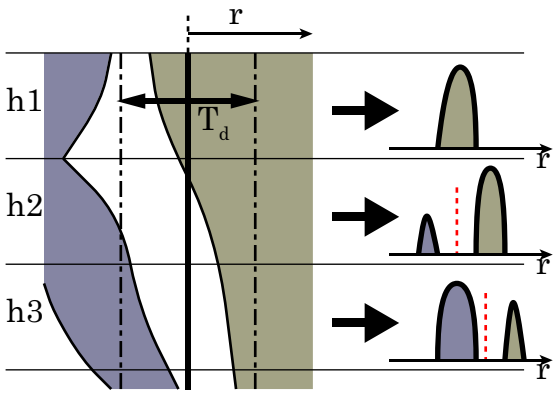

(b) Local distribution of point-cloud

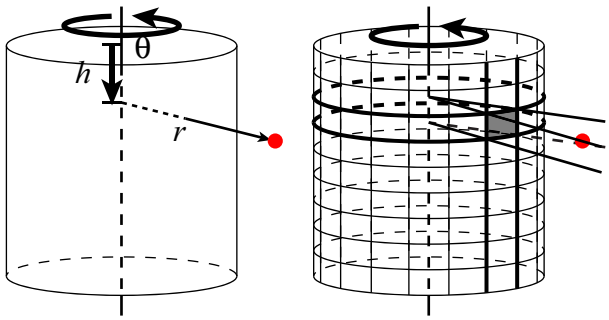

(c) Cylindrical mesh division

Figure 3.4: Segmentation based on distance distributions.

Further segmentation based on neighborhoods

Even if we perform the segmentation based on the local distance distribution, there will still remain some points which are segmented into multiple body components. However, every point in the point-cloud should be segmented uniquely into a single body component except for joints. For performing further segmentation for a point which is segmented into multiple body components, we use the segmentation results of the points within a certain distance (neighborhood points) of the point. There can be the following three cases for a point which is segmented into multiple body components:

1. The point is at a joint and is segmented into the two body components on the two sides of the joint.
2. The point is not at a joint but is segmented into two body components.
3. The point is segmented into three or more body components.

Point at joint segmented into body components on both sides We suppose the points near the joint of two joined body components A and B. In surface reconstruction process, some of such points connect the surfaces of the body components. However, such points could also lead to cause invalid surfaces. Therefore, it is desirable that the point-cloud of parts other than joint should be segmented into one of the body components. Whether the point belongs to a joint or not is decided as follows based on the segmentation results of the neighbor points. The segmenting destination of the point is determined to be body component A (B) in the following cases.

- All neighbor points are segmented into A (B), as depicted in Figure 3.5(a).
- Some neighbor points are segmented into A (B) and the rest are segmented into both A and B, as depicted in Figure 3.5(b).

For the case as depicted in Figure 3.5(c), namely, that

- there are three kinds of neighbor points: the points segmented into A, those segmented into B, and those segmented into both A and B,

the procedure is as follows. If the neighbor points segmented into both are sufficiently few, they are segmented into both and retained as ‘junction’.

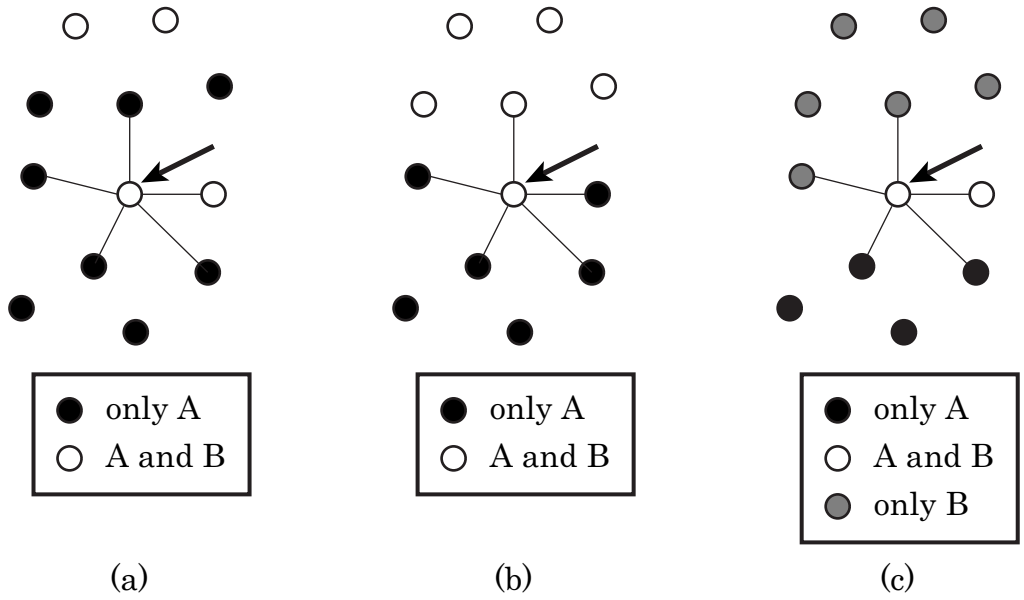

Figure 3.5: Segmentation of points belong to two components of body around the joint: (a) Neighbor points segmented only into A; (b) Neighbor points segmented into A or into both; (c) Neighbor points segmented into A, into B, or into both.

When there are many neighbor points which are segmented to both, we process the other points first. Then the body component into which the neighbor points are segmented is determined again, and the segmenting destination is determined according to the situation of the neighbor points.

Points other than at joints segmented into two body components The points which are segmented into two body components, but are not at a joint will cause problems in distortion correction and surface reconstruction. Such points should be segmented into one of the body components.

We determine the segmenting destination for each point which is segmented into two body components A and B based on the distances between each of the neighbor points and both the model surface of A and B. Firstly, For a point segmented into two body components, we calculate the distances d_A and d_B to the model surfaces of body components A and B, respectively. Secondly, we calculate the distance from each of the neighbor points which are segmented into only one of body components A and B to its segmented

component (A or B). Thirdly, we calculate average distance from neighbors to their components as d'_A and d'_B, respectively. Finally, the point which is segmented into two body components A and B is segmented into the body component with the smaller value of $|d_A - d'_A|$ and $|d_B - d'_B|$.

Points segmented into three or more body components Points segmented into three or more body components can be generated in various cases, such as when a joint is close to another body component, or when multiple joints are close together. In order to handle these various cases in a unified way, we reduce the number of body components which the point is segmented into to two or less by the following procedure.

Let a point segmented into three or more body components be denoted by p. For the point p_1 closest to p, we investigate the number of body components into which it is segmented. If the number of body components into which p_1 is segmented is less than that of p, point p is segmented into the same body components as point p_1, since it is assumable that neighbor points are similarly segmented into body components. The above procedure is iteratively applied until there are no more points segmented into three or more body components. When the number of destination body components for segmentation is at most two, further segmentation is performed as described before.

3.3 Overcoming time consuming disadvantage

With the method in Section 3.2, we can segment the whole point-cloud into body component. The point-cloud of each component would be distorted by the motion of the component. When we consider the segmented point-cloud separately, the subject is assumable as a rigid object and we can take another approach which is not speeding up the measurement. The position of points which is acquired by light stripe triangulation would be changed by the rigid motion of the subject. This motion distorts the shape acquired by light stripe triangulation. By acquiring the rigid motion during the scanning, we can correct the distortion in acquired shape by calculating the original position of each point. In this section, we discuss a method of correcting distortion by supposing each body component as single moving rigid object.

3.3.1 Distortion mechanism

First of all, we figure out the distortion mechanism in shape measurement by light stripe triangulation. We denote the sensor coordinate system which is fixed to the sensor equipment as Σ^e. In the case of light stripe triangulation, the shape of the subject is acquired as the point-cloud which is expressed in Σ^e. Since we can acquire the shape from only part of the subject at a moment by the light stripe triangulation, we acquire the whole shape as integrating the partial shapes which are acquired for some moments. When the subject is rigid and stays still, the shape and position of whole subject is always same in Σ^e. Therefore, in conventional light stripe triangulation, the whole shape of the subject is acquired as integrated the partial shapes in Σ^e without any regard.

In the case of that the subject is single moving rigid object, the shape of the object is always same, however the position of the object will be changed in Σ^e. Although the partial shape which is acquired at a moment is not distorted, it would be changed its position by object's motion. Integrating the partial shapes without any regard for changing the position will cause the distortion in whole shape, which is acquired as integrated the partial shapes.

3.3.2 Distortion correction

Here, we introduce another coordinate system which is fixed to the subject, and we denote it as the object coordinate system, Σ^o. Since Σ^o is fixed to the subject, both the shape and position of the subject is always same in Σ^o. Therefore, if the integration of the partial shape is performed in Σ^o, we can acquire distortion-free shape of the object. In order to performing the integration in Σ^o, we need to transform the point-cloud from Σ^e to Σ^o.

Distortion correction is performed by using the transformation from Σ^e to Σ^o at moment t, which is denoted as $\boldsymbol{W}(t)$, as follows:

$$\boldsymbol{p}^o_{t,n} = \boldsymbol{W}(t)\boldsymbol{p}^e_{t,n}. \tag{3.1}$$

Here, $\boldsymbol{p}^e_{t,n}$ and $\boldsymbol{p}^o_{t,n}$ $(n = 1, \cdots, N_t)$ denote the position of a point of the point-cloud, which is acquired by light stripe triangulation at moment t and consists of N_t points, in Σ^e and Σ^o respectively. $\boldsymbol{W}(t)$ is rigid transformation, which has 6 DOF (degrees of freedom). $\boldsymbol{p}^e_{t,n}$ and $\boldsymbol{p}^o_{t,n}$ can be expressed as a 4x1 column vector in homogeneous coordinates, and $\boldsymbol{W}(t)$ can be also expressed

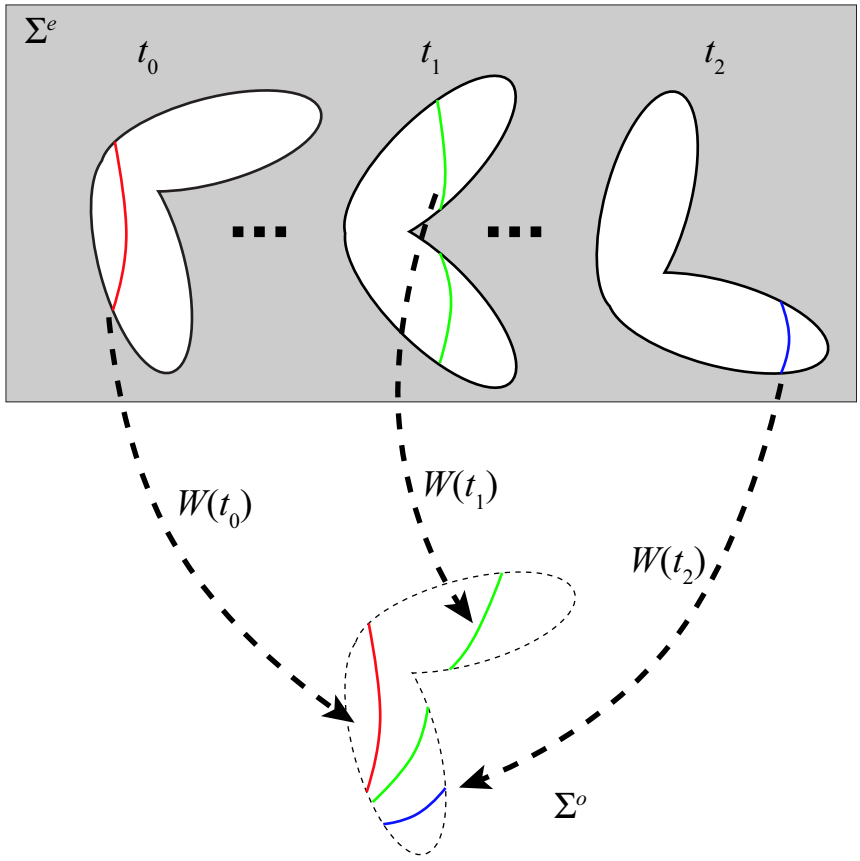

Figure 3.6: Distortion correction for single moving rigid object.

as a 4x4 matrix. We can acquire undistorted shape of a single moving rigid subject by integrating all $\boldsymbol{p}^o_{t,n}$ at every t as depicted in Figure 3.6.

3.4 Overcoming discreteness disadvantage

In this section, we present a method of the surface reconstruction for the point-cloud which is segmented into the component. Except for the fingers and the toes, which have detailed structures, the components of the human body can be considered to have shapes similar to cylinders or elliptic cylinders.

It is assumed that the surface of the body components is composed of a

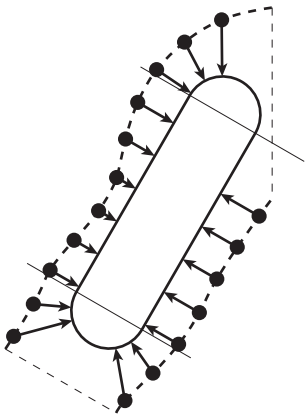

Figure 3.7: Projecting point-cloud onto surface.

cylindrical surface surrounding the main axis and hemispheres closing both ends. We estimate the main axis of the point-cloud by using PCA (principal component analysis) and project the point-cloud of each component onto the two-dimensional surface, and construct two-dimensional Delaunay net among the point-cloud on projected surfaces. We reconstruct the surface by applying the connectivity of the Delaunay net to the point-cloud in the original three-dimensional space. We project the point-cloud of each component on the surfaces of a cylinder and hemispheres as depicted in Figure 3.7.

3.4.1 Projection onto cylindrical surface

In order to project the points of point-cloud onto the cylindrical surface, a cylindrical coordinate system (r, θ, h), is defined as in Section 3.2.2. We denote the component along the axis of the cylinder as h, the distance from the cylinder surface as r, and the angle on the plane perpendicular to the axis of the cylinder as θ $(0 \leq \theta \leq 2\pi)$ as depicted in Figure 3.7 (a). The direction of the angle $(\theta = 0)$ is set arbitrarily. The point at (r, θ, h) is projected onto (R, θ, h) (Figure 3.7 (b)). Here, R is the radius of the cylindrical surface for projection. Letting $u = R\theta$ and $v = h$, the point projected onto the cylindrical surface is represented in 2D coordinates (u, v) as depicted in Figure 3.7 (c).

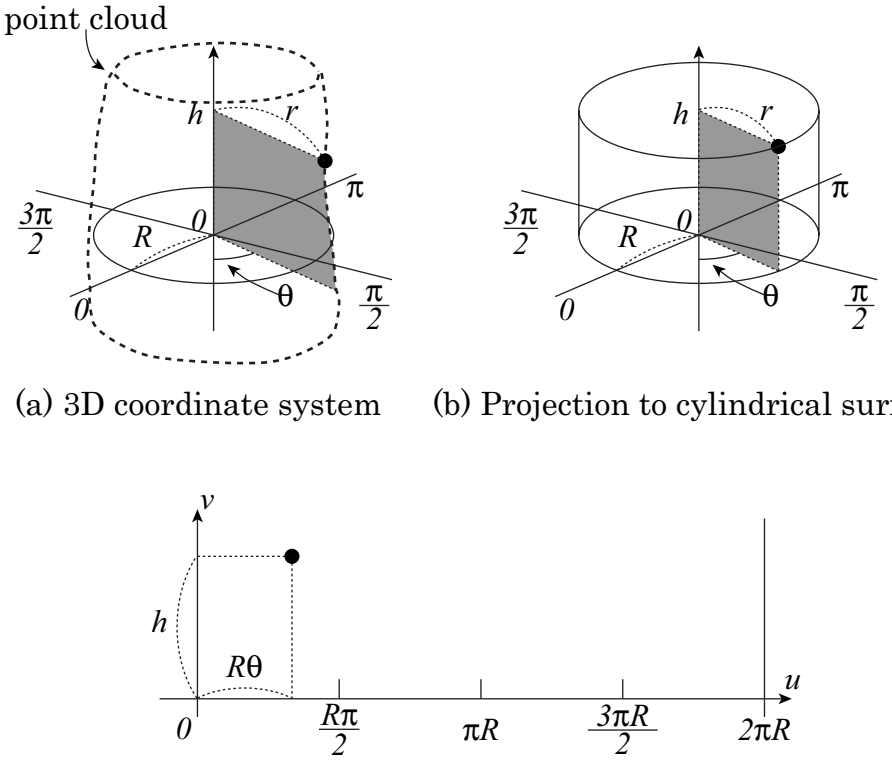

(a) 3D coordinate system (b) Projection to cylindrical surface

(c) 2D coordinate system on cylindrical surface

Figure 3.8: Projection to cylindrical surface.

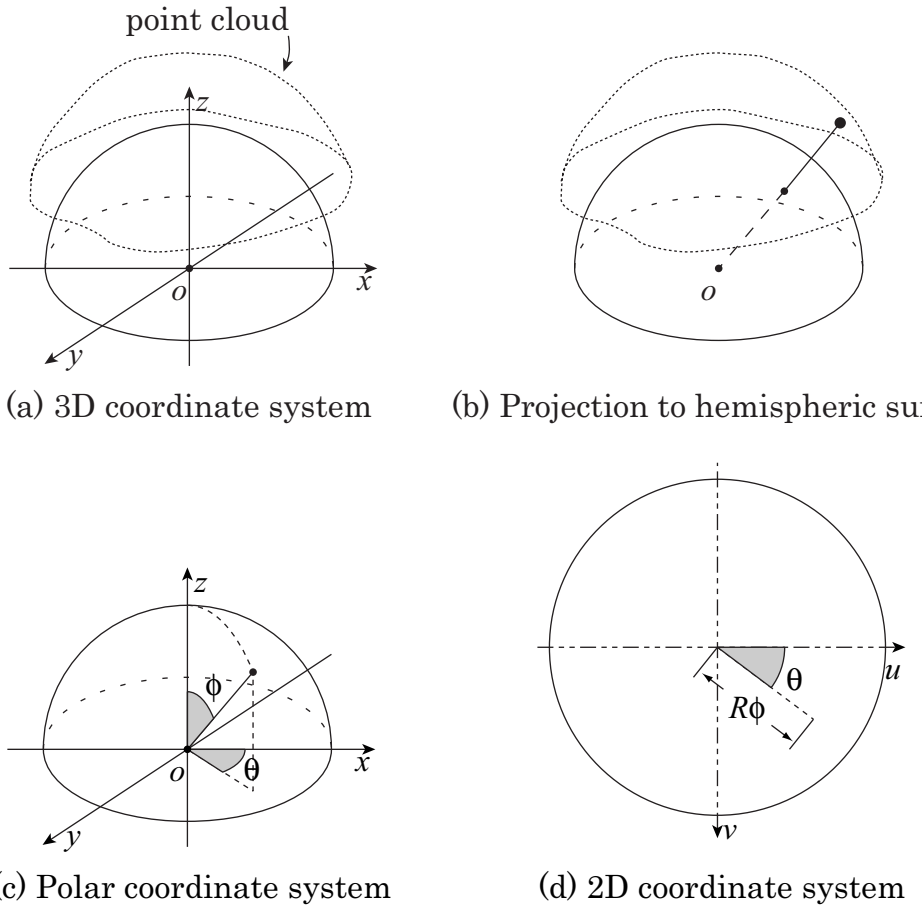

(a) 3D coordinate system (b) Projection to hemispheric surface

(c) Polar coordinate system (d) 2D coordinate system

Figure 3.9: Projection to hemispherical surface.

3.4.2 Projection onto hemisphere

We project the points onto the hemispherical surface which is represented in the three-dimensional polar coordinates (r, θ, ϕ), with the center of the hemisphere as the origin as depicted in Figure 3.7 (a). The point at (r, θ, ϕ) is projected onto (R, θ, ϕ) (Figure 3.7 (b)). Here, R is the radius of the hemispherical surface for projection. Using the θ and ϕ of the point on the projected hemispherical surface as depicted in Figure 3.7 (c), the 2D coordinates (u, v) are defined as $u = R\cos\theta$ and $v = R\sin\theta$ as depicted in Figure 3.7 (d).

3.4.3 Making continuous surface

In order to reconstruct the surface for the point-cloud, we construct two-dimensional Delaunay net among the projected point-cloud and applying the connectivity of the Delaunay net to the point-cloud in the original three-dimensional space.

Since we divide the point-cloud into two or more groups according to the shape of the surface in order to project the points into cylindrical surface or hemispherical surface, a Delaunay net is constructed separately for each of them. In order to avoid that the constructed surface is separated, the range of projection onto the cylindrical surface is expanded so that the area of projection onto the hemispherical surface and the area of projection onto the cylindrical surface overlap in the course of projection. Then, we delete the overlapping surface, which would be superfluous. A similar situation arises when Delaunay nets are constructed for the point cloud projected onto a cylindrical surface. On the two-dimensional surface of the cylinder, the two ends ($\theta = 0$ and $\theta = 2\pi$) represent the same position in three-dimensional space. The points which lie near $\theta = 0$ or $\theta = 2\pi = 0$ are near in three-dimensional space, however are separated in the projected surface. Without any regard, a Delaunay net is constructed separately. In order to solve this problem, we project the points near $\theta = 0$ into the neighborhood of $\theta = 2\pi$ and vice versa, and delete the overlapping surface after constructing the surface.

3.5 Experiments and results of segmentation

In this section, we show experiments of segmenting the acquired point-cloud of the subject who will make an effort to maintain a posture. We prepared synthetic data and real data for the experiment, and segmented them into body component by applying the proposed method.

3.5.1 Experiments with synthetic data

Synthesizing point-cloud

We simulate the light stripe triangulation for making some synthetic point-clouds in various postures, which have some holes in occluded area from laser or cameras. As the subject, we used synthesized articulated human

model of the Poser3 software (Meta Creations Co.), which constructs three-dimensional patch models of the human shape in the standing posture and other postures (10 in all). We placed cameras at the front and the rear of the patch models and projected the laser sheet from the angle of $k\pi/12(k = 1, 2, 3)$. We suppose that the resolution of the camera is approximately 10mm near the body surface. Figure 3.10 shows the example of synthetic point-clouds, where simulation was applied to some postures by setting $k = 1$. The expanded figures indicate that the point-cloud has holes at the arms and legs.

Applying the proposed method to synthetic data

As an experiment, we performed segmentation for the synthetic data by applying the proposed method.

Firstly, we estimated the posture of the point-cloud by the method described in Section 3.2.1 to estimate the posture. We constructed the volume model from the point-cloud and matched the articulated body model to that. Then we refine the matching result by using the point-cloud itself. Figure 3.11 shows the results of (a) constructing volume model, (b) matching the articulated body model to the volume model, and (c) refinement of the articulated body model by using the point-cloud. We set the upper limit of the voxel size as 40mm, and the weight of the contour voxels as 2. The results show that we can correctly estimate the posture for the synthetic point-cloud. It is also verified that by correcting the results of matching using the point-cloud, the length and width of the body sections are adjusted and the error is decreased.

Next, we performed segmentation based on the result of posture estimation. For comparison, we performed simple segmentation as described at the beginning of Section 3.2.2, and proposed method. Figure 3.12 shows the results of segmentation for the point-cloud of standing posture. We set the threshold T_d as 30% of the width of each body component model. We set the number of mesh divisions for (θ, h) as 6 and 8, and the threshold T_n as the maximum frequency of the point-cloud in the mesh, multiplied by 0.05.

The results shows that although the segmentation would be failed in the simple method using the threshold as indicated with circle in the figure, the proposed method segments the point-cloud correctly. The points under the armpits were segmented into both of the chest and the upper arm in the results of simple segmentation. It would cause problems in distortion correc-

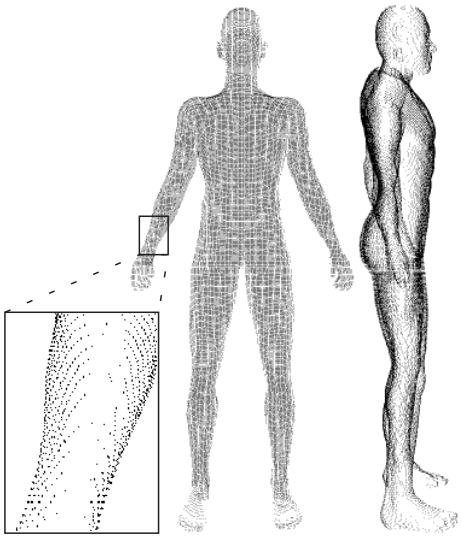

(a) Standing posture

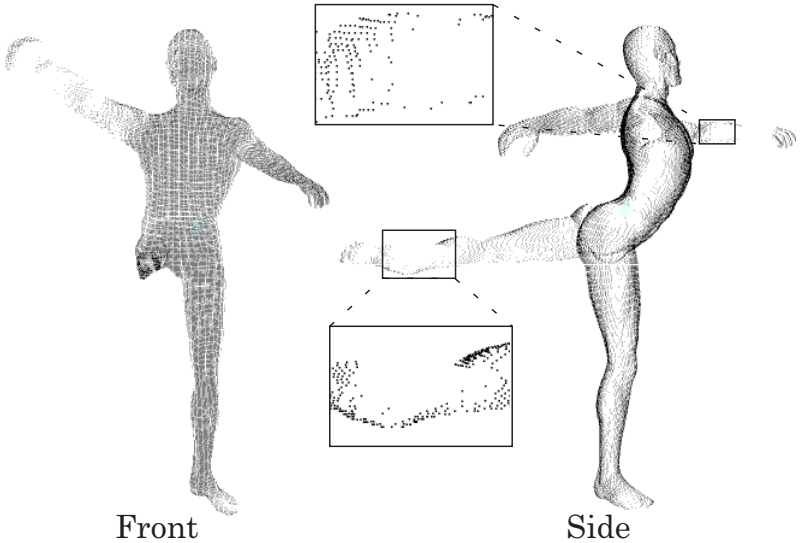

(b) Arabesque (ballet posture)

Figure 3.10: Synthetic point-cloud.

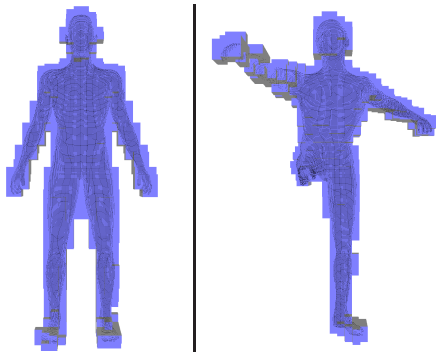

(a) Constructed volume data

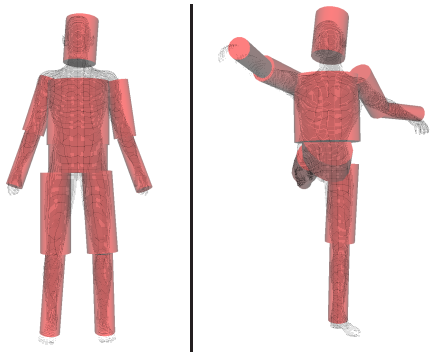

(b) Model matching with volume data

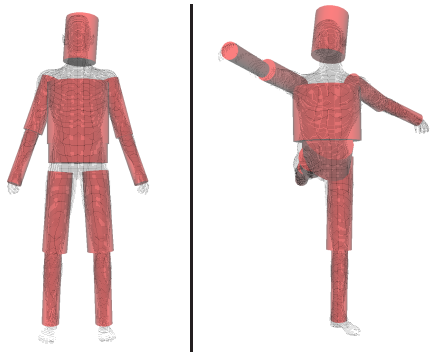

(c) Refinement with point-cloud

Figure 3.11: Posture estimation for synthetic data.

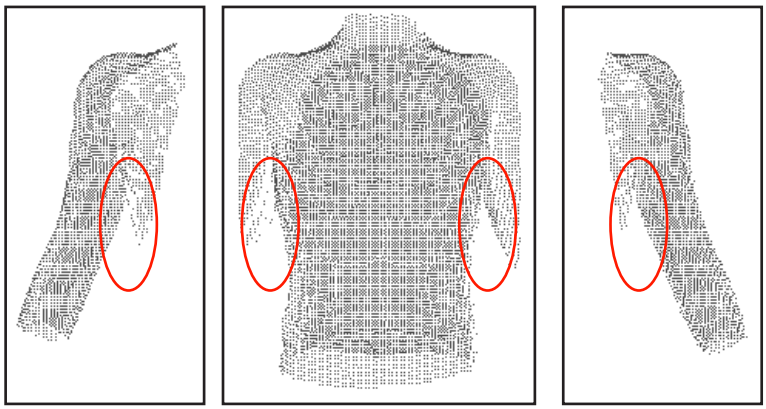

(a) Results of single segmentation

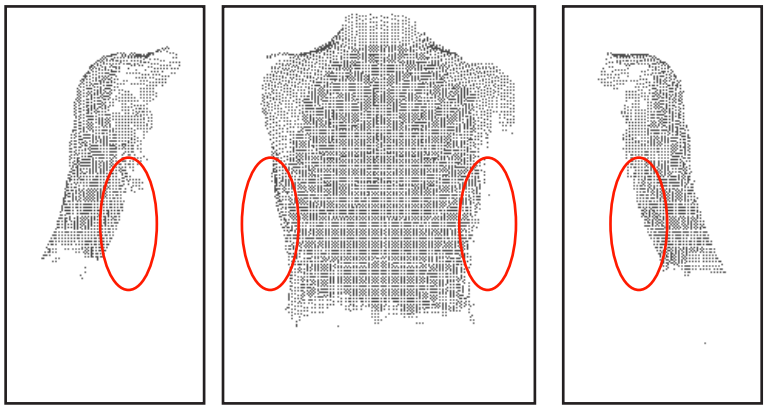

(b) Results of proposed method

Figure 3.12: Segmentation results.

tion, and invalid surfaces which fill the armpit in the surface reconstruction as described in Figure 3.13(a). Meanwhile, such points are correctly segmented in the results of proposed method and we could reconstruct surface without invalid surfaces for the point-cloud as described in Figure 3.13(b).

For remaining synthetic data in various postures, we could also estimate the posture and perform the segmentation correctly.

3.5.2 Experiments with real data

Performing measurement

We measured a real human body and applied proposed method to the acquired point-cloud. We used the conventional measurement system which has accuracy of 1.0mm and a resolution of 2.0 mm. Since the conventional measurement system does not measure the rigid transformation of body components during the laser scanning, we cannot correcting distortion in the acquired data. Figure 3.14 shows the acquired data from measuring the subject in standing posture and the other posture.

Applying the proposed method to real data

We applied the proposed method of segmentation to the acquired point-clouds. Figure 3.15 shows the results of segmentation for the point-cloud by using simple segmentation and the proposed method. Despite the point-cloud would be little distorted by the subject's trunk sway, the point-cloud was correctly segmented into each body component. However, the point-cloud acquired from real measurement includes some unnecessary points which do not correspond to the subject's surface in reality. Although the proposed method could kick out some of them, the proposed method cannot eliminate such points completely. Remaining of them could cause problem in correcting distortion and would produce invalid surface in surface reconstruction. Such points should be eliminated by using another method as pre-processing.

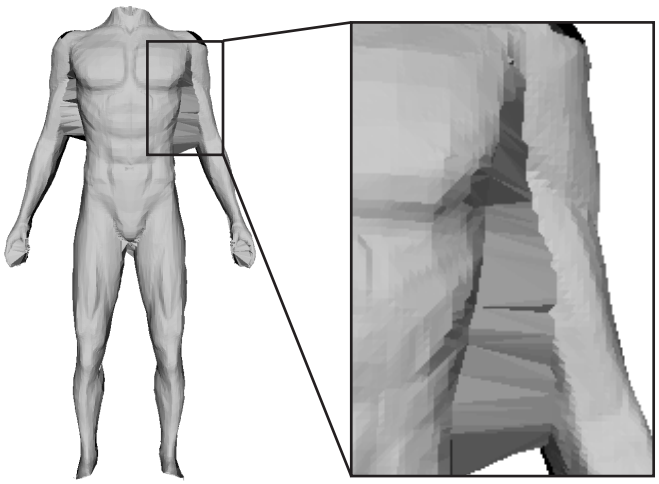

(a) Reconstructed surface based on simple segmentation

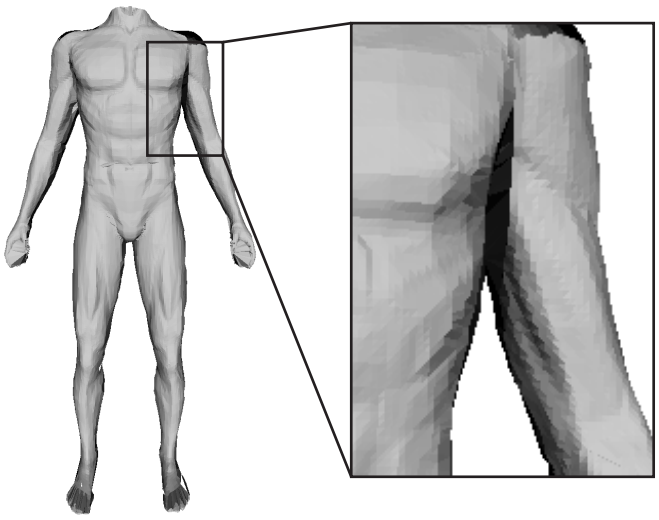

(b) Reconstructed surface based on proposed segmentation

Figure 3.13: Reconstructed surface based on segmentation results.

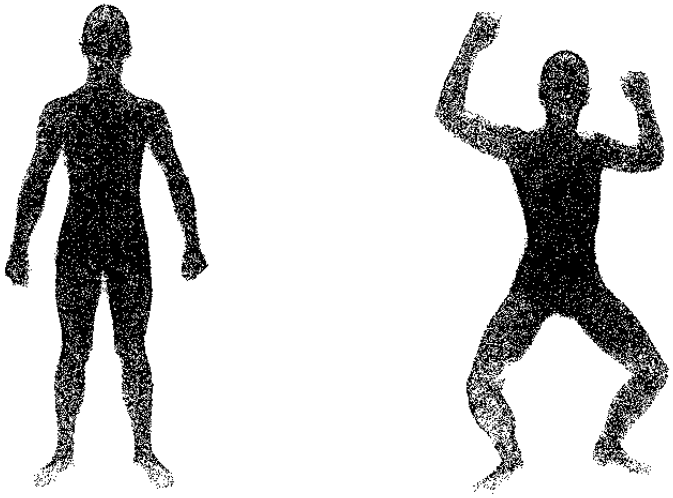

(a) Standing posture (b) Victory posture

Figure 3.14: Point-cloud obtained from real measurement.

3.6 Experiments and results of correcting distortion

In Section 3.5, although we have presented the validity of the method of segmentation and surface reconstruction, we couldn't evaluate the method of distortion correction. Therefore, we empirically present the validity of distortion correction in this section.

We evaluate the accuracy of light stripe triangulation and distortion correction in human body measurement. In order to evaluate the accuracy, we need to compare the acquired shape with distortion-free shape. However, we cannot acquire the distortion-free shape of human body by light stripe triangulation.

For acquiring both shapes, we put a lot of markers on the subject and acquire their three-dimensional position by stereo vision, not light stripe triangulation. We can measure the three-dimensional position of markers from multiple images at a moment, and these are free from distortion due to the subject's motion. In order to acquire distorted shape, we simulate light stripe triangulation by using markers' positions during a certain time. Furthermore, we correct the distortion in distorted shape, and evaluate our

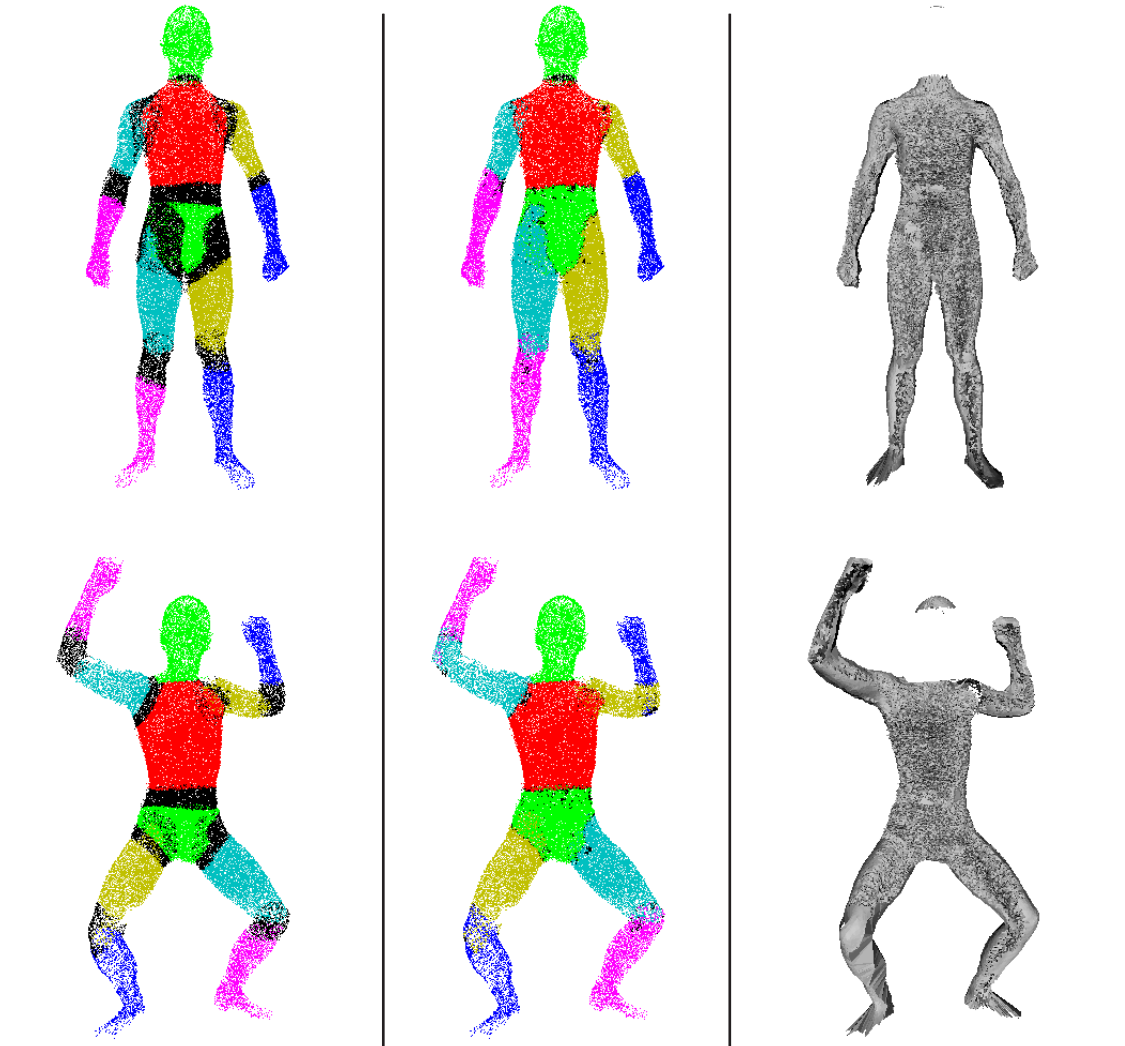

(a) Simple segmentation (b) Proposed method (c) Reconstructed surface

Figure 3.15: Segmentation results for real measurement.

method by comparing the undistorted shape and distortion-free shape. In order to correct the distortion, we need to acquire rigid transformation and segmentation. For acquiring the rigid transformation, we estimate rigid motion of the subject by using the markers' positions. We perform segmentation manually in this experiment for evaluating accuracy strictly.

We evaluate 3 kinds of accuracy in this experiment:

1. Rigidity of the human body segments.
2. Accuracy of the light stripe triangulation (with distortion).
3. Accuracy of our method.

Furthermore, in order to demonstrate the shape distortion and distortion correction, we actually perform shape measurement by light stripe triangulation distortion correction for a part of human body and applying our method to the distorted shape.

3.6.1 Methodology

Marker position acquisition

In this experiment, we put N markers M_n on the subject and measure their three-dimensional position $\boldsymbol{M}_n(t)$ at moments $t = 0, \cdots, T$. We observe the subject by multiple of synchronized and calibrated cameras and calculate three-dimensional position of markers by using stereo vision, is the same as *triangulation* (see also Figure 3.16).

In order to calculate $\boldsymbol{M}_n(t)$, we need the two-dimensional position of each M_n on each camera image, $I^i(t)$, and the correspondence of two-dimensional markers' position among the cameras. We denote the two-dimensional position of M_n on $I^i(t)$ as $\boldsymbol{m}_n^i(t)$.

In this experiment, we track the markers on sequence of images for each camera $I^i(t)$ to get two-dimensional markers' position, $\boldsymbol{m}_n^i(t)$. We give the position $\boldsymbol{m}_n^i(0)$ for all M_n on the initial frame $I^i(0)$ of each camera manually. For other frames $I^i(t)$, $\boldsymbol{m}_n^i(t)$ are estimated sequentially from their pixel value at $\boldsymbol{m}_n^i(t-1)$ on $I^i(t-1)$ and the pixel values around $\boldsymbol{m}_n^i(t-1)$ on $I^i(t)$. $\boldsymbol{m}_n^i(t)$ is estimated as the center of the area that has values similar to the pixel value of $\boldsymbol{m}_n^i(t-1)$ on $I^i(t-1)$. We also give the correspondences of the markers among cameras manually. Then, we can calculate makers' three-dimensional positions $\boldsymbol{M}_n(t)$.

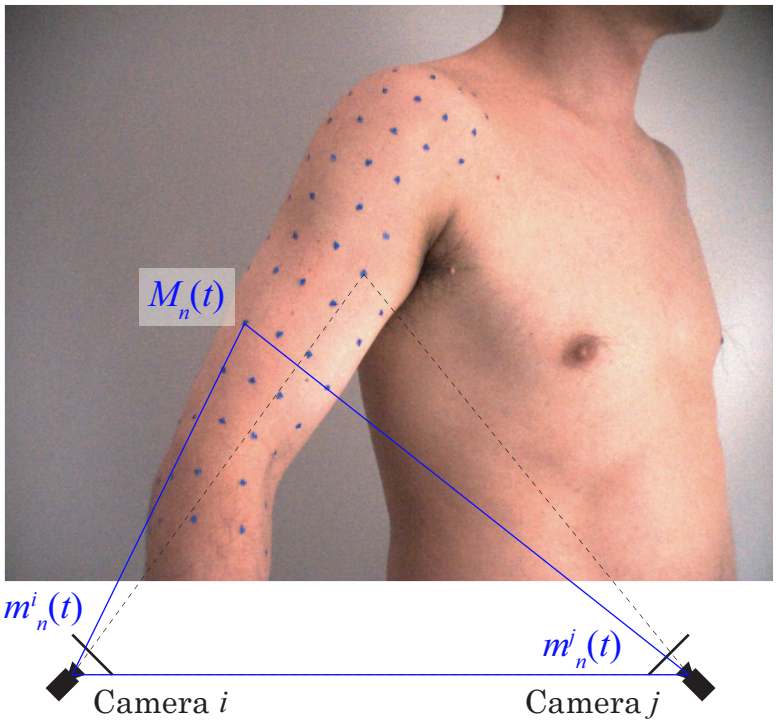

Figure 3.16: Marker observation by multiple cameras for experiment.

In order to performing triangulation, the pose of cameras is also required. We employ Zhang's method [36] and the factorization method [30] for acquiring the pose of cameras.

If the cameras are appropriately arranged for observing all markers by more than two cameras, three-dimensional position of all markers are calculable at every moment. A set of measured markers' position $\boldsymbol{M}_n(t)$ at a moment t is free from the distortion which is caused by the subject's motion. We take it as a distortion-free shape of the subject.

Evaluation of rigidity

We consider sets of markers' position, $\boldsymbol{M}_n(t)$ and $\boldsymbol{M}_n(t')$, which are acquired at t and t' respectively. If there is no error in marker measurement and the subject is completely rigid, although $\boldsymbol{M}_n(t)$ and $\boldsymbol{M}_n(t')$ in the sensor coordinate system Σ^e are changed over time due to the subject's motion, $\boldsymbol{M}_n(t)$ and $\boldsymbol{M}_n(t')$ in the object coordinate system Σ^o are not changed as discussed in Section 3.3. From the equation 3.1, the following equation is satisfied at any moment:

$$\begin{aligned} \boldsymbol{W}(t)\boldsymbol{M}_n(t) &= \boldsymbol{W}(t')\boldsymbol{M}_n(t') \\ \boldsymbol{M}_n(t') &= \boldsymbol{W}^{-1}(t')\boldsymbol{W}(t)\boldsymbol{M}_n(t) \\ &= \boldsymbol{D}_{t,t'}\boldsymbol{M}_n(t) \end{aligned} \tag{3.2}$$

Here, $\boldsymbol{D}_{t,t'}$ represents the motion of the subject from t to t'.

As mentioned above, if there is no error in marker measurement and the subject is completely rigid, we can conform the set of $\boldsymbol{M}_n(t)$ to the set of $\boldsymbol{M}_n(t')$ with appropriate rigid transformation. We consider the error function $E(\boldsymbol{D})$ for acquiring the rigid transformation:

$$E(\boldsymbol{D}) = \frac{1}{N}\sum_{n=1}^{N} ||\boldsymbol{M}_n(t') - \boldsymbol{D}\boldsymbol{M}_n(t)|| \tag{3.3}$$

Here, N is the number of markers and $\boldsymbol{D}$ is a rigid transformation matrix which is defined by 6 parameters. With appropriate rigid transformation $\boldsymbol{D}_{t,t'}$, $E(\boldsymbol{D}_{t,t'})$ shall be 0, however, $E(\boldsymbol{D})$ will never be 0 in reality since there is error in marker measurement and the human body component have a little deformation over time. Therefore, $\boldsymbol{D}_{t,t'}$ is estimated as the $\boldsymbol{D}$ that minimizes $E(\boldsymbol{D})$. We estimate $\boldsymbol{D}_{t,t'}$ by using the Powell minimization algorithm [23].

The residual $E(\boldsymbol{D}_{t,t'})$ represents the measurement error of markers and the non-rigidity of human body components. We evaluate the non-rigidity as an average residual $\overline{E}$, which is defined as follows:

$$\overline{E} = \frac{1}{T(T+1)} \sum_{t=0}^{T} \sum_{\substack{t'=0 \\ t' \neq t}}^{T} E(\boldsymbol{D}_{t,t'}). \tag{3.4}$$

We can evaluate only the non-rigidity of human body components by comparing the $\overline{E}$ of human body components with $\overline{E}$ of actual rigid object, $\overline{E'}$.

Simulation of light stripe triangulation

We simulate the measurement of light stripe triangulation and acquire the markers' position on the distorted shape, $\widehat{\boldsymbol{M}_n}$, by using the sets of markers' positions $\boldsymbol{M}_n(t)$ which are acquired during $t = [0, T]$.

The simulation is performed using a pair of sequences of images, $I^C(t)$ and $I^L(t)$, from two cameras C and L which observe marker' position. If a laser sheet which goes through lens center of the camera L scans the object, the stripe on the subject is observed as a straight line on camera image $I^L(t)$. Here, the laser plane is parallel to the x-axis of the image plane of camera L and the laser is scanned along the y-axis going from $y = 0$ on the image plane at $t = 0$ to $y = 1$ at $t = T$. The stripe at t is observed as the line of $y = t/T$ $(0 \leq x \leq 1, 0 \leq y \leq 1)$ in the camera image $I^L(t)$ (see Figure 3.17). Therefore, the observation of the laser scanning from the camera L is done by integrating the lines from a sequence of the images $I^L(t)$ into a single image, which we call the integrated scanline image $\widehat{I^L}$ (see also Figure 3.18).

With the integrated scanline image $\widehat{I^L}$, we can simulate the markers position, $\widehat{\boldsymbol{M}_n}$, on the acquired shape using the light stripe triangulation. When the marker M_n is observed on $\widehat{I^L}$ at coordinate $\widehat{\boldsymbol{m}_n^L} = (\widehat{x}_n^L, \widehat{y}_n^L)$, $\widehat{\boldsymbol{M}_n}$ is given by $\boldsymbol{M}_n(\widehat{y}_n^L/T)$ since the marker would be illuminated by the laser sheet at $t = \widehat{y}_n^L/T$. For all t, $\boldsymbol{M}_n(t)$ is obtained using the pair of sequences of images $I^C(t)$ and $I^L(t)$, so $\widehat{\boldsymbol{M}_n}$ can also be acquired. Using $\widehat{\boldsymbol{M}_n}$ and $\boldsymbol{M}_n(t)$, we evaluate the accuracy of the light stripe triangulation for a trunk swaying

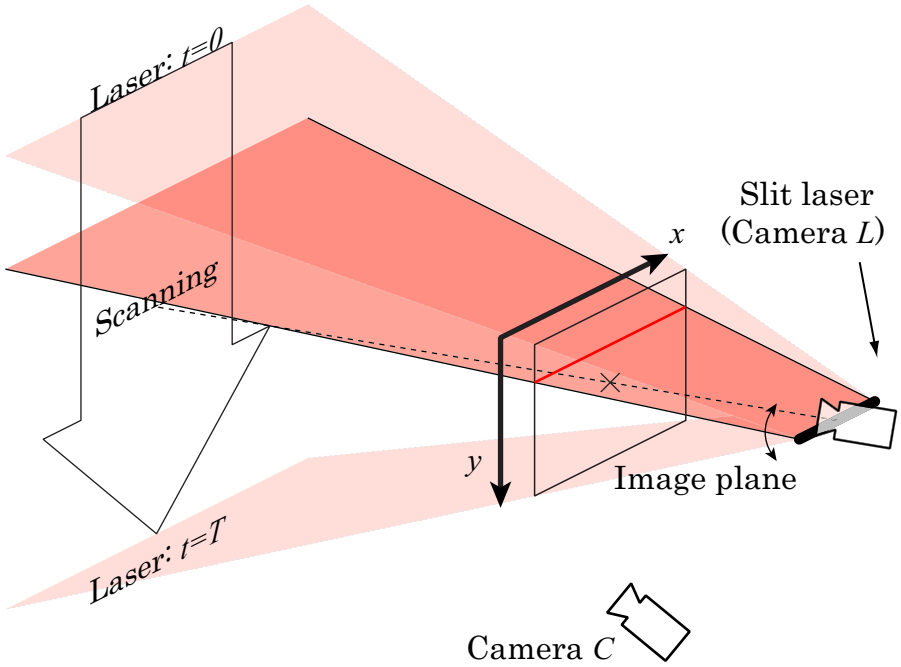

Figure 3.17: Laser stripe simulation by using two cameras.

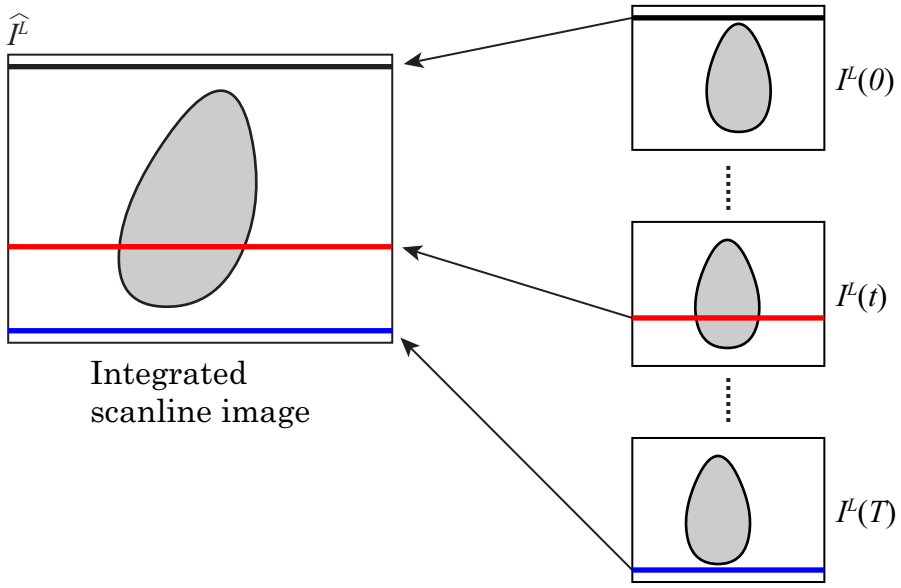

Figure 3.18: Scanline integration from the sequence of camera images.

subject, $\widehat{E}(t)$, as follows:

$$\begin{aligned}\widehat{E}(t) &= \frac{1}{N}\sum_{n=1}^{N}||\widehat{\boldsymbol{M}_n} - \boldsymbol{M}_n(t)|| \\ &= \frac{1}{N}\sum_{n=1}^{N}||\boldsymbol{M}_n(\widehat{y}_n^L/T) - \boldsymbol{M}_n(t)||. \end{aligned} \tag{3.5}$$

Experiment of distortion correction

To evaluate the accuracy of the measurement with distortion correction, we correct the distorted shape $\widehat{\boldsymbol{M}_n}$. We estimate the rigid transformation by using the positions of only 3 of N markers, and evaluate the accuracy of the method by using the other $N-3$ markers. Firstly, we calculate the estimate of the rigid transformation matrix $\widetilde{\boldsymbol{D}_{t,0}}$ from 3 markers' positions $\boldsymbol{M}_n(t)$ as estimated with equation 3.3. Then, we transform markers $\widehat{\boldsymbol{M}_n}$ into their corrected position at $t=0$, $\widetilde{\boldsymbol{M}_n(0)}$, as follows:

$$\begin{aligned}\widetilde{\boldsymbol{M}_n(0)} &= \widetilde{\boldsymbol{D}_{\widehat{y}_n^L/T,0}}\widehat{\boldsymbol{M}_n} \\ &= \widetilde{\boldsymbol{D}_{\widehat{y}_n^L/T,0}}\boldsymbol{M}_n(\widehat{y}_n^L/T). \end{aligned} \tag{3.6}$$

Finally, we evaluate the accuracy, $\widetilde{E}$, by comparing $\widetilde{\boldsymbol{M}_n(0)}$ and $\boldsymbol{M}_n(0)$ as follows:

$$\widetilde{E} = \frac{1}{N}\sum_{n=1}^{N}||\widetilde{\boldsymbol{M}_n(0)} - \boldsymbol{M}_n(0)||. \tag{3.7}$$

3.6.2 Exprimental results of accuracy and discussion

Firstly, we show the result of evaluating the measurement error of markers. We put fifty-eight 3-mm-square markers on a mannequin (completely rigid subject) with about 20mm grid spacing (see Figure 3.19-a), and measure their 3D position for 10 seconds with 15fps cameras, that is $T=150$. Figure 3.19-b illustrates the markers position with wire-frame at $t=18, 123$. We calculated the marker measurement accuracy from all pairs of time t, $\overline{E'}$ was 0.73mm. Figure 3.19-c also illustrates markers position at $t=123$ transformed into markers at $t=18$ using the estimated rigid transformation matrix. This figure shows that the rigid transformation matrix is estimated properly.

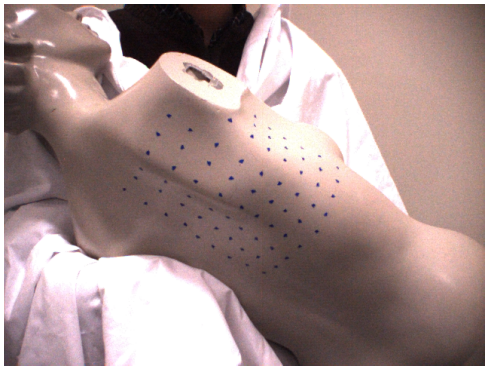

(a) Rigid object to be subject (mannequin).

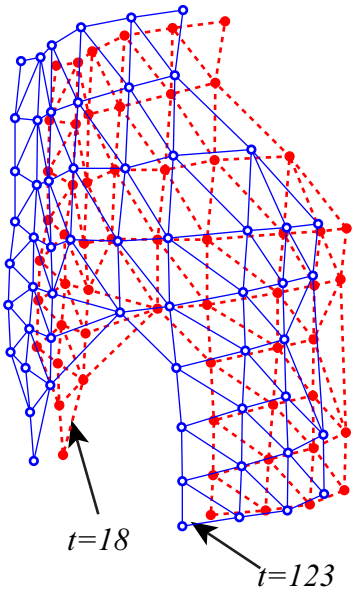

(b) Acquired markers' positions.

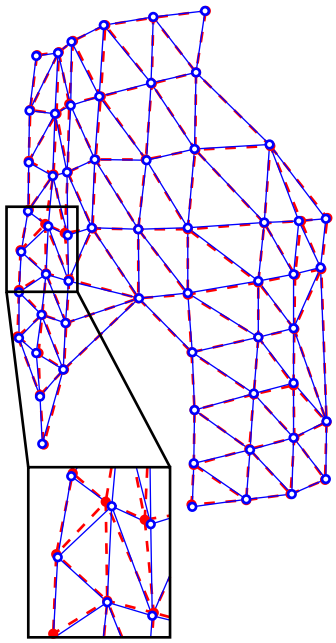

(c) Transformed markers' position

Figure 3.19: Experimental result for the rigid subject.

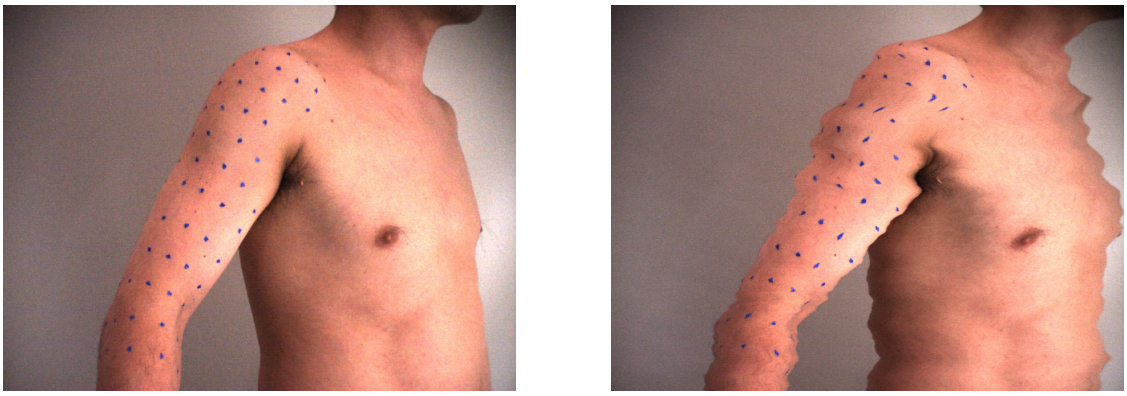

(a) Acquired camera image at *t=0*. (b) Integrated scanline image.

Figure 3.20: Experimental result of integrated scanline image.

Next, we show the result of evaluating the non-rigidity of human body components $\overline{E}$, the accuracy of the light stripe triangulation $\widehat{E}(t)$ and the accuracy of the proposed method $\widetilde{E}$. Here, we assume that the human body consists of rigid components as follows:head, breast, waist and right and left upper arms, forearms, thighs and legs. As mentioned above, we put about 70 markers on the breast and waist, and about 30 markers on the head, upper arms, forearms, thighs and legs and measured the markers' positions for 30 seconds, $T = 450$. Although the subject makes an effort to keep standing still for avoiding the distortion during the measurement in this experiment, there will be trunk sway, which distorts the shape which is acquired by the light stripe triangulation.

We show the camera image at $t = 0$, $I^L(0)$, and the integrated scanline image $\widehat{I^L}$ from an upper arm observation in Figure 3.20. Figure 3.20 shows how the trunk sway of the subject will distort the acquired shape.

To evaluate the accuracy, we measure the markers' position at $t = 0$, $\boldsymbol{M}_n(0)$, the markers' position acquired with simulated the light stripe triangulation, $\widehat{\boldsymbol{M}_n}$, and the positions as corrected by the proposed method, $\widetilde{\boldsymbol{M}_n(0)}$. Figure 3.21 illustrates acquired sets of markers' position $\boldsymbol{M}_n(0)$, $\widehat{\boldsymbol{M}_n}$, $\widetilde{\boldsymbol{M}_n(0)}$ as measured from Figure 3.20. We chose 3 markers to estimate rigid motion (the black markers in Figure 3.21) and evaluate the accuracy of the correction using the remaining markers (the white markers).

We show the $\overline{E}$, $\widehat{E}(0)$ and $\widetilde{E}$ calculated for each component of the body

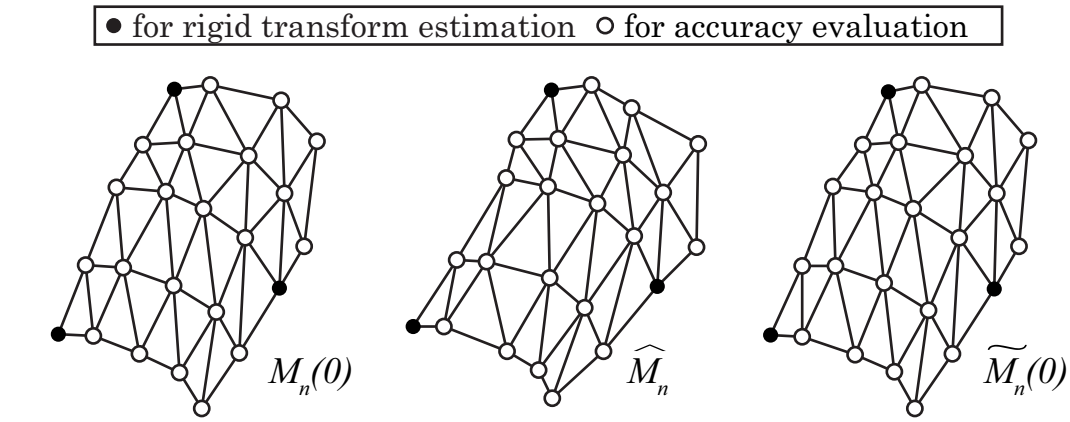

Figure 3.21: Experimental results of marker measurement.

in Table 3.1. From the results, we conclude that:

- When the subject makes an effort to maintain the posture, each component of the body will deform non-rigidly less than about 1mm ($\overline{E}$).
- Even if the subject makes an effort to maintain the posture, the motion of the body degrades the measurement accuracy $\widehat{E}(0)$ to about 10mm.
- The proposed method maintains the accuracy within about 2mm ($\widetilde{E}$) with distortion correction.

Although this experiment was performed in the case that the subject makes an effort to maintain the posture for avoiding the distortion during the measurement, there is serious distortion in the shape which is acquired by light stripe triangulation.

3.6.3 Experiments of shape measurement

We show the acquired shape of a right upper arm and breast with two methods, the light stripe triangulation and the proposed method. In order to acquire the rigid transformation of the right upper arm and breast, we put 4 markers on each component and measure its three-dimensional positions at every moment by synchronized and calibrated cameras. We reconstruct the surface from acquired point-cloud by making Delaunay mesh.

Table 3.1: Evaluation for different body-parts (unit:mm).

Component	Rigidity $\overline{E}$	Distortion $\widehat{E}(0)$	Proposed method $\widetilde{E}$
head	0.69	10.32	1.09
breast	0.70	7.48	1.47
waist	0.89	6.56	1.56
upper arm	1.54	31.50	1.86
forearm	1.14	7.16	1.99
thigh	1.16	3.94	1.25
leg	1.87	3.35	2.64
Average	1.14	10.04	1.69

Figure 3.22 illustrates the shape acquired with the light stripe triangulation and the result of the proposed method. The distortion which we can see in encircled area of Figure 3.22-a is corrected by the proposed method, Figure 3.22-b.

3.7 Conclusion

In this chapter, we supposed that the subject will make an effort to maintain the posture, and propose the methods of modeling human body.

Firstly, we presented the method of segmenting the point-cloud into body component. We supposed that the point-cloud is distorted a little and forms almost human body under the assumption that the subject will make an effort to maintain its posture during the measurement. We performed segmentation by two procedures. The first procedure is estimating the posture of the point-cloud by matching the articulated body model to the point-cloud. The second procedure is segmenting the point-cloud based on the local distance distribution on the model surface and neighborhoods information.

Secondly, we presented the method of correcting the distortion. After performing the segmentation, we can treat segmented point-cloud of each body component as the distorted shape acquired from single moving rigid object. We can simply correct the distortion by transforming each points based on the motion of the body component.

Thirdly, we presented the method of reconstructing surface. By reconstructing the surface for each body component separately, we can acquire

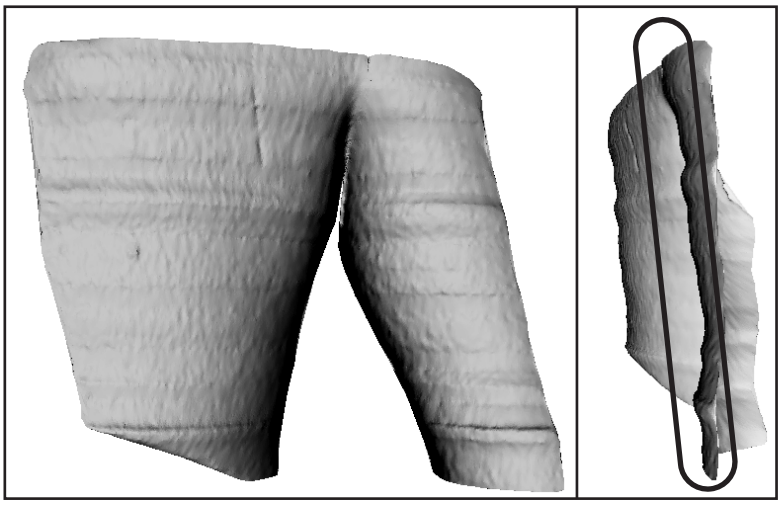

(a) Distorted shape acquired by light stripe triangulation

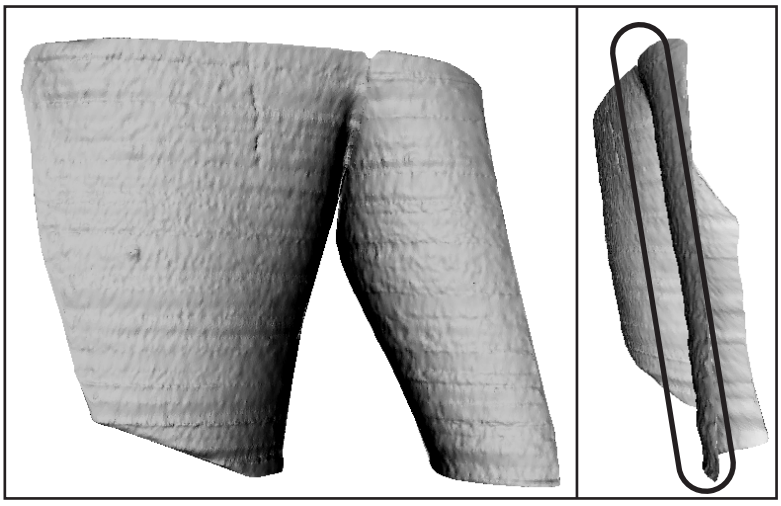

(b) Undistorted shape by our method

Figure 3.22: Comparison of contemporary and proposed method for shape reconstruction.

the surface of whole body without invalid surfaces. We performed surface reconstruction of each body component by projecting the point-cloud onto the cylindrical or hemispherical surface and constructing the Delaunay net on it.

We performed the experiments of segmentation and surface reconstruction for synthetic data and real data. The results show that the methods correctly estimate the posture, segment the point-cloud into each body segment, and reconstruct the surface for any postures.

We also performed the experiments of evaluating the validity of distortion correction. We presented how each component of the human body undergoes less than 1mm of non-rigid deformation when the subject makes an effort for to maintain the posture. Nevertheless, experimental results show that the accuracy of the light stripe triangulation is degraded from less than 1mm of error to about 10mm distortion due to the motion of human body. The method corrects the distortion with about 2mm accuracy in spite of the subject motion during the measurement.

Chapter 4

Human body modeling of moving subject

4.1 Introduction

In this chapter, we suppose that the measurement is performed with the second approach for overcoming 'incompleteness' mentioned in Section 1.2.2, and discuss a method of human body modeling. The approach supposes that the subject variously changes its posture during the measurement. As discussed in Chapter 3, we need to segment the point-cloud into body components for overcoming both of 'time consuming' disadvantage and 'discreteness' disadvantage.

Since the subject changes its posture variously during the measurement, it is supposed that the point-cloud would be catastrophically distorted and it does not form human body. Therefore, we cannot take the approach of estimating the posture to segment the point-cloud which discussed in Chapter 3.

Since it is difficult to segment seriously distorted point-cloud, we propose a method of segmentation which incorporates the distortion correction. Firstly, we correct the distortion without segmentation as if whole point-cloud belongs to each body component. Since whole point-cloud includes the points which belong to the other component, such points form superfluous shape, which we denote as '*false shape*'. Secondly, we perform the segmentation as detecting such false shape. We tackle the problem of detecting the false shape under the assumption that every body component does

not change its shape even if the subject changes its posture. Based on the assumption, we find the changed part with changing subject's posture for each body component. We denote whole of such part as '*nonexistent area*'. We determine the points which are in nonexistent area as false shape. The points which are not detected as false shape are to be segmented into the body component.

In order to acquire the nonexistent area for each body component, we additionally observe the silhouette of whole subject and the transformation of each body component at the same time. We can perform this observation by using the cameras which is used in light stripe triangulation with controlling lighting environment.

4.2 Distortion correction without segmentation

4.2.1 Distortion correction for multiple rigid objects

In Section 3.3.2, we discuss the distortion correction for single moving rigid object. However, we suppose that there are multiple of moving rigid objects. We figure out correcting distortion in shape measurement for multiple rigid objects by light stripe triangulation. Here, we denote the number of objects as S.

For single of moving rigid object, we denoted the rigid transformation at moment t as $\boldsymbol{W}(t)$. Similarly, in the case of multiple of moving rigid objects, we denote the rigid transformations of each moving object $s(:= 1, \cdots, S)$ at moment t, as $\boldsymbol{W}^s(t)$. As in the case for single object, we consider the sensor coordinate system Σ^e. While, we need to consider S object coordinate systems, Σ^{o_s} for every object $s(:= 1, \cdots, S)$. Each $\boldsymbol{W}^s(t)$ is defined as the transformation from Σ^e to Σ^{o_s} at t.

In order to performing distortion correction, we need to acquire the origin of each point of point-cloud: which object is the point acquired from? In the case that the subject is single object, all points of point-cloud are acquired from only one object. However, in the case that the subject is multiple objects, not all points of point-cloud are acquired from only one object of the components of the subject. Some points of point-cloud are acquired from an object s, other points will be acquired from other object which is not s. The points which are acquired from an object s at a moment t would

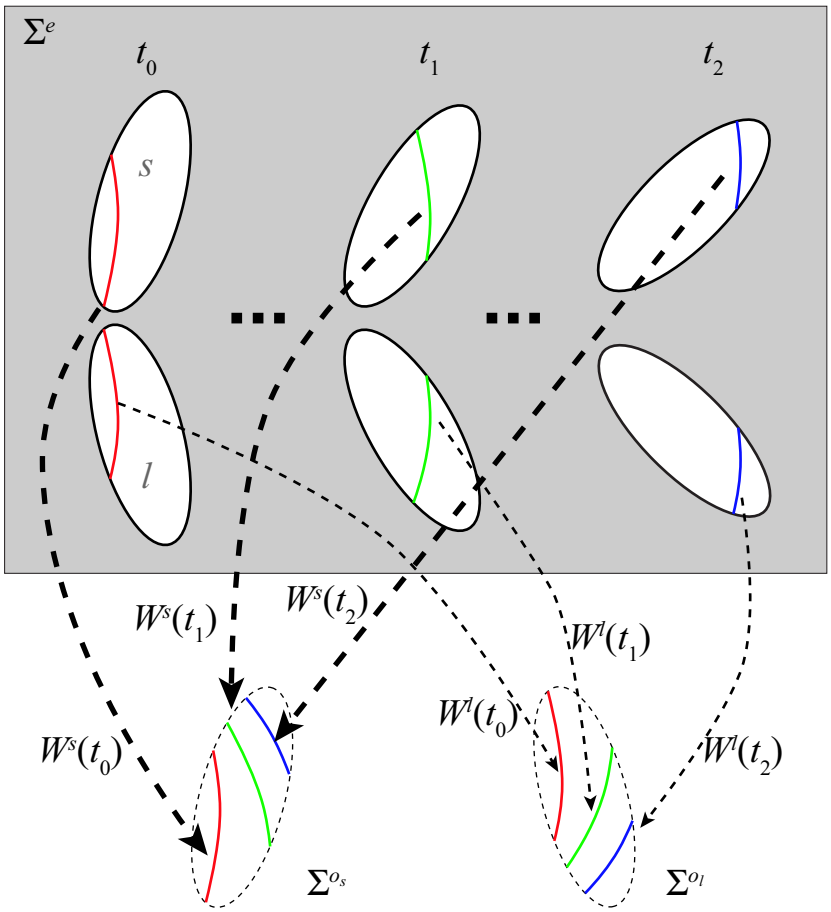

Figure 4.1: Distortion correction for multiple moving rigid objects.

change its position by rigid transformation of object s at t, therefore their position need to be transformed by $\boldsymbol{W}^s(t)$, as depicted in Figure 4.1. In order to performing distortion correction for measuring multiple of moving rigid objects, we need to acquire not only the rigid transformations $\boldsymbol{W}^s(t)$ of every object at every moment, but also the origin of each point of point-cloud.

4.2.2 False shape

If we correct the distortion without segmentation, a problem will occur. We consider that we transform whole point-cloud $\boldsymbol{p}^e_{t,n}$ into coordinate system Σ^{o_s}

of object s by $\boldsymbol{W}^s(t)$. Whole point-cloud includes not only the points which are acquired from the object s, but also the points which are acquired from the other objects. The transformed points which are acquired from object s will form distortion-free shape of the object s. However, the transformed points which are acquired from the other objects will form a shape which does not exist in reality (see also Figure 4.2). We call this superfluous shape as 'false shape'.

4.3 Performing segmentation

4.3.1 Acquiring nonexistent area

We consider the three-dimensional space where there are multiple of moving objects. In the sensor coordinate system Σ^e, the space where the whole subject occupies will change with time as depicted in Figure 4.3(a). Meanwhile, in a coordinate system Σ^{o_s} of object s, the object s keeps occupying the same space and the space where the other objects occupy will change with time. However, the other objects which differently move with s will change their occupancy with time. Therefore, in Σ^{o_s} of object s, there is not included within the object s where the whole subject does not occupy even at a moment for some moments (see also Figure 4.3(b)). We call such area as 'nonexistent area' of object s. Since the part which is acquired from object s will not be in nonexistent area of object s, the points which are in nonexistent area of object s would be from the other objects, and they are detected as false shape.

The nonexistent area of each object s is acquired by using the occupancy of whole subject in Σ^{o_s}, which is transformed occupancy in Σ^e by $\boldsymbol{W}^s(t)$, over time. However, we cannot acquire complete occupancy of the subject in three-dimensional space from any observations, that is to say, complete shape of the subject. Nonetheless, we can acquire some information about spatial occupancies of the subject from observations, and it is not necessary for acquiring the nonexistent area to use complete occupancy of the subject at any moments. It is enough to observe that every area in the nonexistent area is not occupied by the subject for even a moment.

In the proposed method, we acquire the nonexistent area by using the information about spatial occupancy which comes from silhouette of the subject. In order to acquire adequate nonexistent area, we need some silhouettes

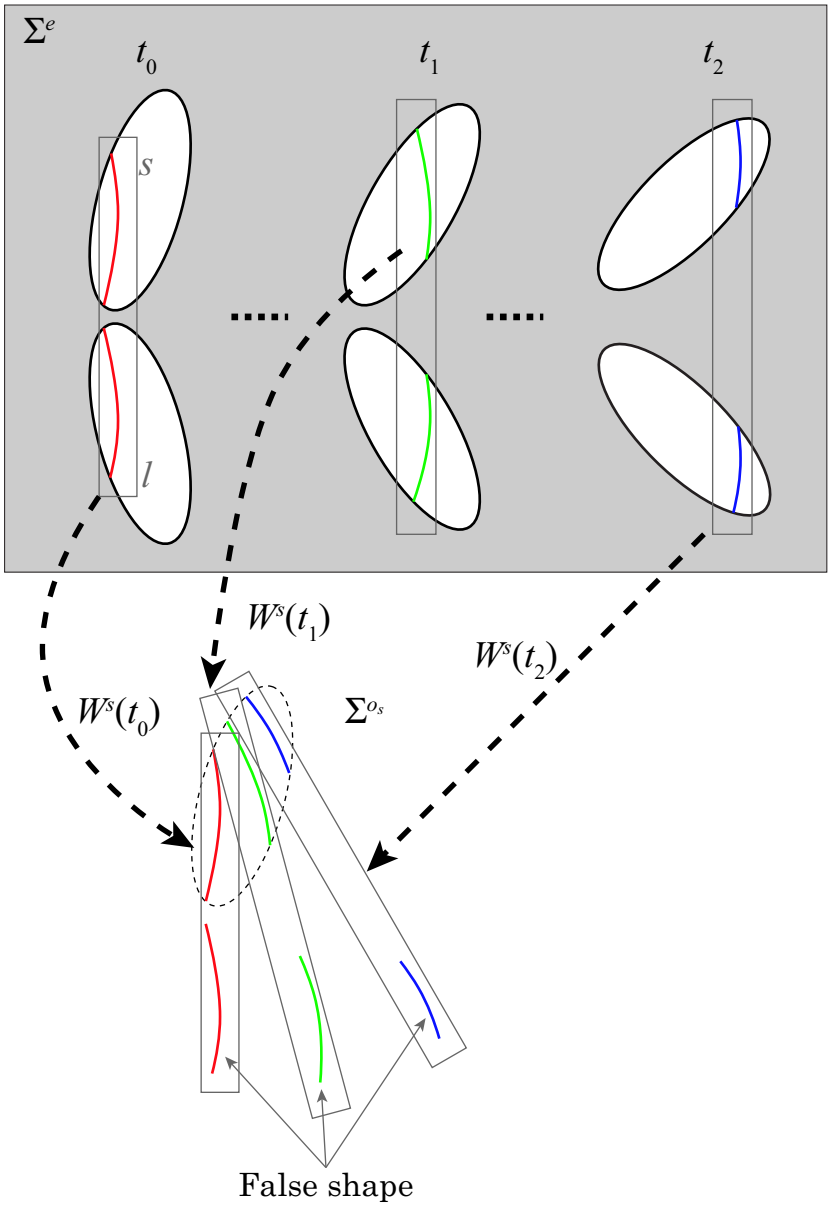

Figure 4.2: False shape appearance.

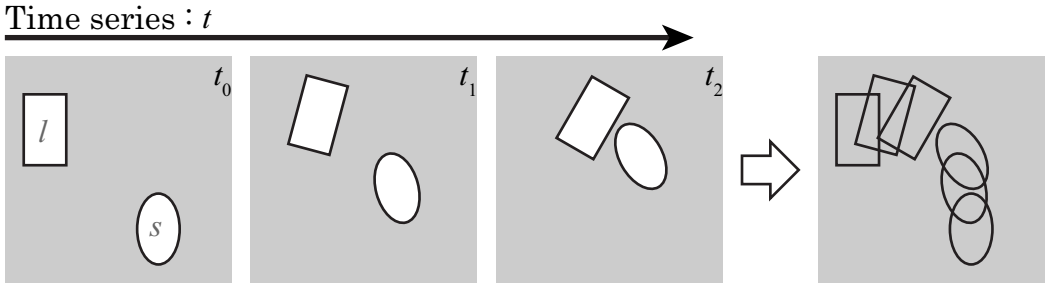

(a) In the equipment coordinate system Σ^e

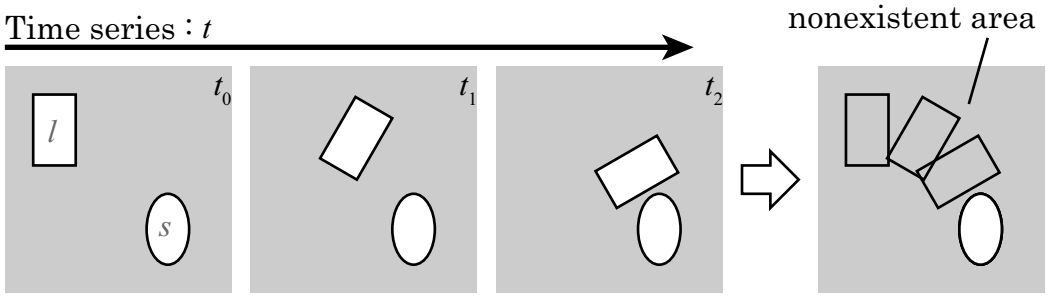

(b) In the object coordinate system Σ^{o_s}

Figure 4.3: Nonexistent area acquisition.

which provide incomplete spatial occupancies for some moments. We discuss acquiring spatial occupancy information in followings.

Acquiring spatial occupancy information in light stripe triangulation

Here, we discuss the spatial occupancy acquired in light stripe triangulation. As discussed in Section 2.1, we observe the subject where is illuminated by the laser sheet with cameras. When we suppose that there is no reflective object such as mirror, we can acquire the information of spatial occupancy as follows:

- there does not exist any objects between the laser source and the subject where is illuminated by the laser sheet
- there does not exist any objects between the camera and the subject where is illuminated by the laser sheet.

We can acquire only planar area mentioned above from an image in light stripe triangulation as depicted in Figure 4.4. In order to acquire enough nonexistent area, we need to observe and merge a huge amount of such thin area. It is not realistic approach.

Acquiring spatial occupancy information from silhouette

The silhouette is the area of the subject in camera images. Such area will be easily acquired by comparing two images of the scene with the subject (foreground image) and the one without the subject (background image). From the silhouette image, we can acquire the information that the spatial area which is projected onto outside of the silhouette in the image is not occupied by the subject as depicted in Figure 4.5. In comparison with the planar area acquired in light stripe triangulation, the spatial area is cubic so that it is efficient to acquire nonexistent area.

It is ideal that the observation of the silhouette is performed in a bright place for observing the subject with cameras vividly since the silhouette is acquired based on pixel values of camera image. On the contrary, light stripe triangulation should be performed in a dark place to detect only the light stripe clearly for measuring the shape accurately. The desirable environments for each observation are conflict.

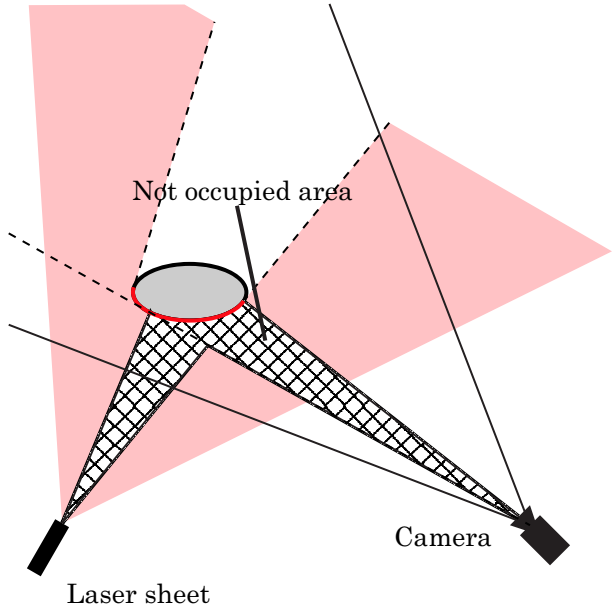

Figure 4.4: Spatial occupancy information in light stripe triangulation.

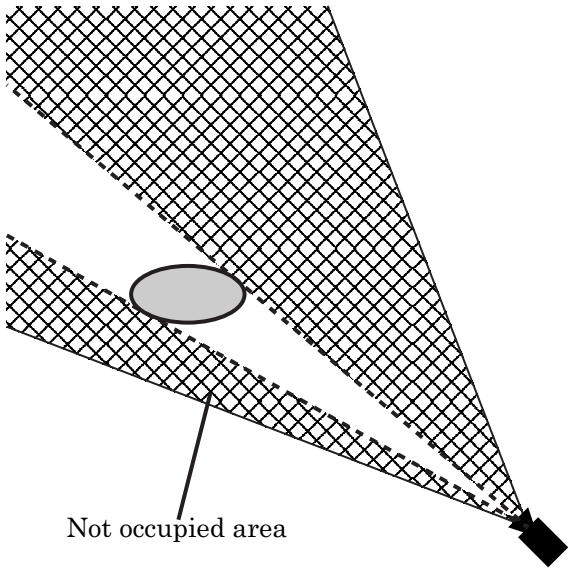

Figure 4.5: Spatial occupancy information from a silhouette image.

Since the spatial area where there is not occupied is normally acquired in Σ^e, we need to transform it into Σ^{o_s} in order to acquire the nonexistent area for object s, which is expressed in Σ^{o_s}. Hence we need to acquire the transformation from Σ^e to Σ^{o_s} for every objects. This indicates that it is only required to observe the silhouette and to acquire the transformation for every object at the same time, it is not necessary to perform that light stripe triangulation and the silhouette observation at the same time. Therefore, we can easily solve the conflict in observing environments discussed above by controlling the lighting.

4.3.2 False shape detection

We present a method to detect the false shape by using the silhouette images of whole subject.

Firstly, we suppose that whole point-cloud belongs to every body component, and undistort the point-cloud for each component s as depicted in Figure 4.6(a). We denote undistorted points as $\boldsymbol{p}_{t,n}^{o_s}$ which is expressed in Σ^{o_s}.

Secondly, we detect the false shape from $\boldsymbol{p}_{t,n}^{o_s}$ based on the nonexistent area acquired from silhouettes. We suppose that we acquire silhouette of whole subject for some moments t' and the transformations $\boldsymbol{W}^s(t')$ at the moments. According to the discussion about the nonexistent area, if a point of $\boldsymbol{p}_{t,n}^{o_s}$ is projected into inside at least one of the silhouettes, the point is detected as false shape. In order to perform the projection, we transform $\boldsymbol{p}_{t,n}^{o_s}$ from Σ^{o_s} into Σ^e of the silhouette observation by $\boldsymbol{W}^s(t')$. Transformed point-cloud, $\boldsymbol{p}_{t,n}^{e,s}(t')$, which is directly projected into the silhouette, is acquired as follows:

$$\begin{aligned} \boldsymbol{p}_{t,n}^{e,s}(t') &= \boldsymbol{W}^s(t')^{-1}\boldsymbol{p}_{t,n}^{o_s} \\ &= \boldsymbol{W}^s(t')^{-1}\boldsymbol{W}^s(t)\boldsymbol{p}_{t,n}^{e}. \end{aligned} \tag{4.1}$$

We project the point-cloud for each silhouette, and eliminate the points which are detected as false shape from $\boldsymbol{p}_{t,n}^{o_s}$, as depicted in Figure 4.6(b).

4.4 Experiments and results

The method proposed in this chapter is applicable to not only human body measurement, but also any of moving rigid objects. In order to validate the

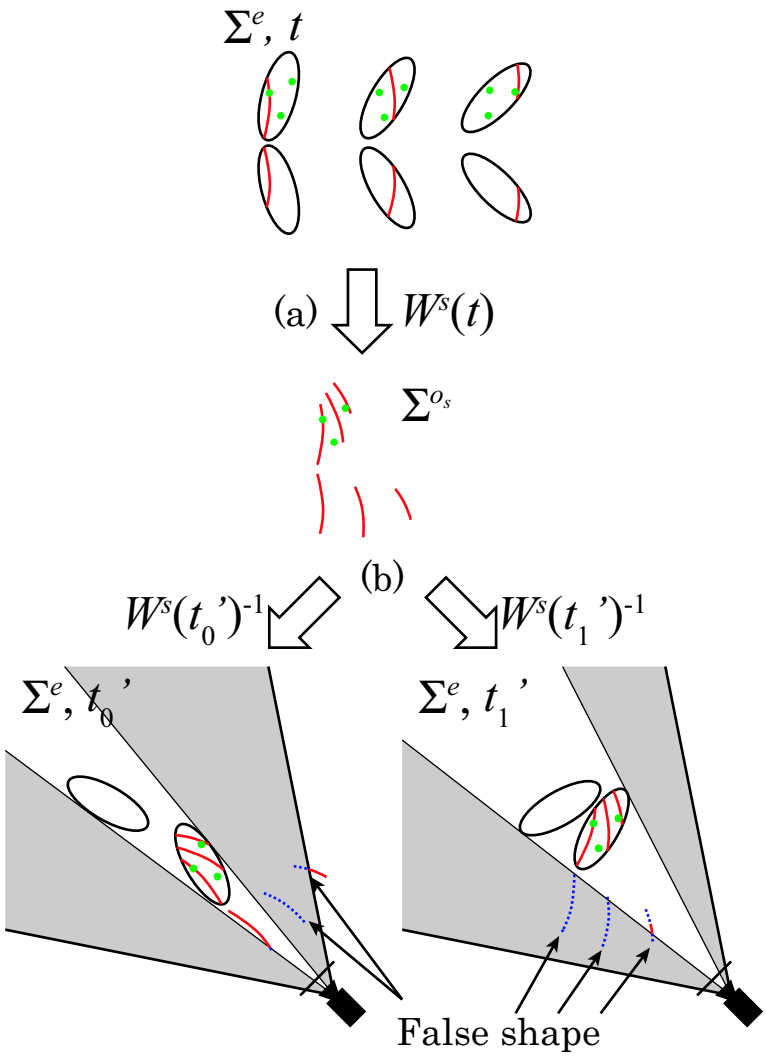

Figure 4.6: An Algorithm of false shape detection.

proposed method, we firstly apply the method to the subject which is able to be segmented obviously. Then, we present the results of measuring the real hand, which we substitute for whole human body. There will be no difference between the hand and the whole body in principle.

4.4.1 Experiment environment

First of all, we present the experimental environment which we implemented for performing light stripe triangulation, silhouette observation, and rigid transformation acquisition. We suppose that the observation area is cubic space about 250mm size and set synchronized 32 cameras around about 1200mm distant from the area.

Light stripe triangulation We set laser scanner beside the observation area. We observed the illuminated part on the subject by the cameras. In order to observe the illuminated part in the camera images vividly, the observation is performed under that the lighting is off.

Silhouette observation We observed the silhouette of the subject by the cameras. In order to observe the whole subject itself in the camera images vividly, the observation is performed under that the lighting is on. As foreground images, we observed the scene with the subject for some moments. And background, we observed the scene without the subject in the same lighting environment. We acquire the silhouettes of the whole subject by comparing the pixel values of foreground images with them of background image.

Rigid transformation acquisition It is requested for the rigid transformation acquisition of all components of the subject that

- it shall not be obstacle to the shape measurement
- it can be performed under both the lighting is on and off
- it can be performed at the same time with both light stripe triangulation and silhouette observation.

In order to realize the acquisition, we utilize the black light and fluorescent markers. We used small sheet marker. It is observable by using cameras

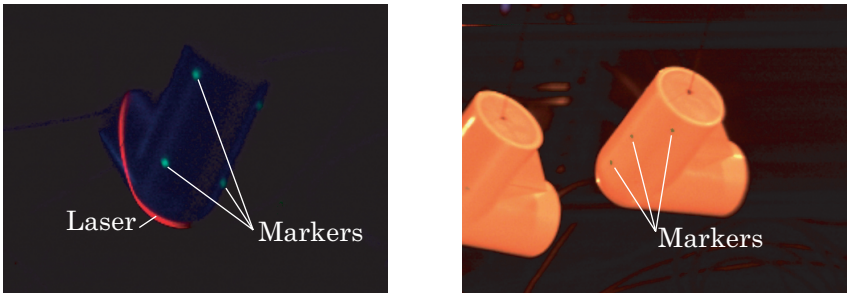

(a) In a dark place (b) In a bright place

Figure 4.7: Marker observation with camera.

however it is not obstacle to the shape measurement. When the lighting is off, even if the black light is on, we can perform the light stripe triangulation since the camera does not observe the illumination on the subject. However, the fluorescent marker emits light which is visible to the camera as presented in Figure 4.7(a). It is also easily observable when the lighting is on as presented in Figure 4.7(b). In order to distinguish the marker from both the laser and the subject, we colored the marker a different color with both the laser and the subject itself.

We put more than 3 markers on the surface for each components of the subject. By using the synchronized and calibrated cameras, we can measure three-dimensional position of markers, and estimate the rigid transformation of each component, as discussed in Section 3.6.1.

4.4.2 Experiment for validating the method

For validating the segmentation of proposed method, we measure rigid objects. We measured a fixed elbow pipe and three moving pipes, which are hanged with thread, by conventional light stripe triangulation.

In each case, we scanned the subject by laser sheet 9 times from different directions. Furthermore, we acquire the silhouette of the subject 9 times at different moments for applying proposed method. Figure 4.8 presents the experimental results. (a) and (b) show an example of the acquired images in light stripe triangulation and silhouette observation, respectively. We estimated the rigid transformations of each objects based on the observed markers in the images for each moment. We show the acquired shape in Σ^e for the fixed pipe by scanning 9 times and the moving pipes by scanning once

Table 4.1: Measurement accuracy evaluation

	Ave.(mm)	Err(mm)	SD(mm)
Fixed pipe	17.14	+0.14	0.20
Moving pipe	16.55	-0.45	0.25

in (c) and (d), respectively. The fixed pipe appeared with its original shape in (c), however three pipes lost their original form due to their movement in (d).

We undistort the point-cloud of moving pipes based on rigid transformation of one of the pipes. (e) presents the acquired shape which is transformed into Σ^{o_s} for one of the pipes. We also show the integrated shapes in Σ^{o_s}, which is acquired by scanning 9 times, in (f). There are undistorted shape and also much false shape which comes from the other pipes.

We applied proposed method to the undistorted shape for detecting the false shape. (g) and (h) presents the result of false shape elimination by applying the proposed method to (e) and (f), respectively. We could acquire undistorted shape for each other pipes without false shape by proposed method.

We also evaluated the accuracy by measuring the radius of the pipes for the acquired shapes of the fixed pipe (c) and a moving pipe (h). We extract the straight parts of the pipe from the acquired shapes, estimate the central axis for them, and calculate the distances between the points and estimated central axis as radiuses. Table 4.1 shows the averages radiuses, its error, and standard deviations of radiuses for the fixed pipe and a moving pipe.

Although the accuracy of the proposed method for measuring the moving objects is little degraded by comparing the conventional method for measuring the fixed subject, the results indicate that the proposed method can acquire undistorted shape for multiple of independently moving rigid objects. The accuracy degradation will occur since the error in measuring with the proposed method includes not only the error in conventional light stripe triangulation, and also the error in estimating the transformation of moving objects.

4.4.3 Hand modeling

As substitute for the human body modeling, we performed hand modeling by measuring the human hand. As for human body, we assume that the human

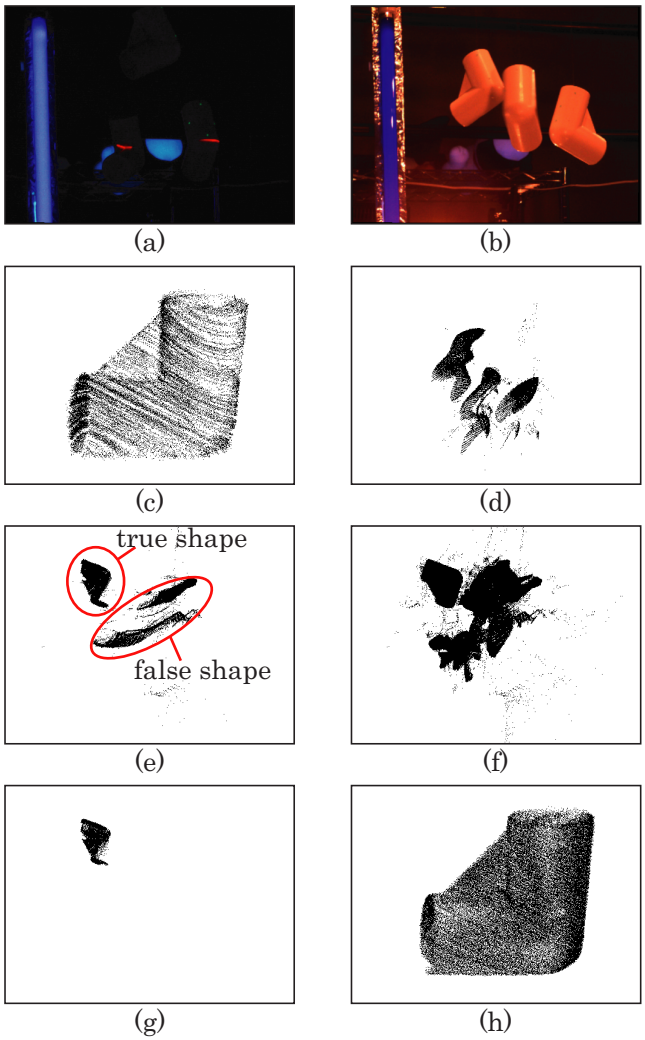

Figure 4.8: Shape measurement for the pipe(s): (a),(b)An acquired image in light stripe triangulation and silhouette observation, respectively; (c),(d) Acquired shape for fixed pipe and moving pipes by conventional measurement; (e),(f)Undistorted shape of one of the pipes with false shape from 1 scan and 9 scans, respectively; (g),(h)Acquired shape from (e),(f) with our method, respectively.

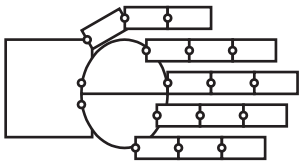

Figure 4.9: Skeletal structure of hand

hand consists of 18 rigid objects as depicted in Figure 4.9.

We measure the shape of hand by light stripe triangulation in 9 postures. We also observe some silhouettes of the hand in other 9 postures. Figure 4.10 presents some of the results of proposed method for measuring the hand. (a) shows an acquired shape in Σ^e by conventional light stripe triangulation for human hand. For each component of the hand, we transformed the acquired shape, which is shown in (a), into Σ^{o_s}, detected the false shape by using the silhouettes of whole hand, and eliminated it. We present the results of proposed method for each component with different color in (b). By integrating the results from measurements in 9 postures, we acquire the whole shape of every component as shown in (c). (d) shows the reconstructed surface model for each component as discussed in Chapter 3.4.

We present the components of acquired hand model in Figure 4.11. We can see that each component overlaps one another, especially around the joint. Although it seems to be superfluous, it enables us to synthesize the hand shape in the other postures.

We synthesize the hand shape in the other posture by transforming each component presented in Figure 4.11. We utilize the rigid transformations of the components, $\boldsymbol{W}^s(t')$, acquired in silhouette observation. Figure 4.12 shows the image of silhouette observations and the synthesized shape of the hand.

4.4.4 Discussion

We will also be able to synthesize the shape of the hand in arbitrary postures by estimating the rigid transformations of the components in the posture. Several methods [15, 24, 19] have been proposed for estimating skeletal structure from motion capture data. Since we acquired the same data as motion capture data in the rigid transformation acquisition, we can also construct the skeletal structure to the acquired hand model. Based on the skeletal

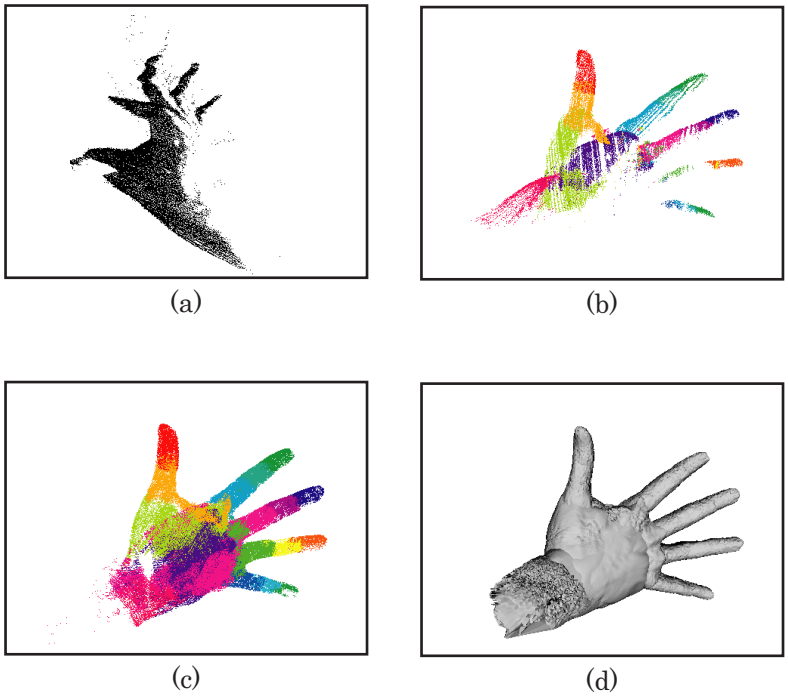

Figure 4.10: Shape measurement for hand: (a)Acquired shape by conventional measurement; (b)Acquired shapes with our method from 1 scan; (c)Acquired shapes with our method from 9 scans; (d)Surface model constructed from (c).

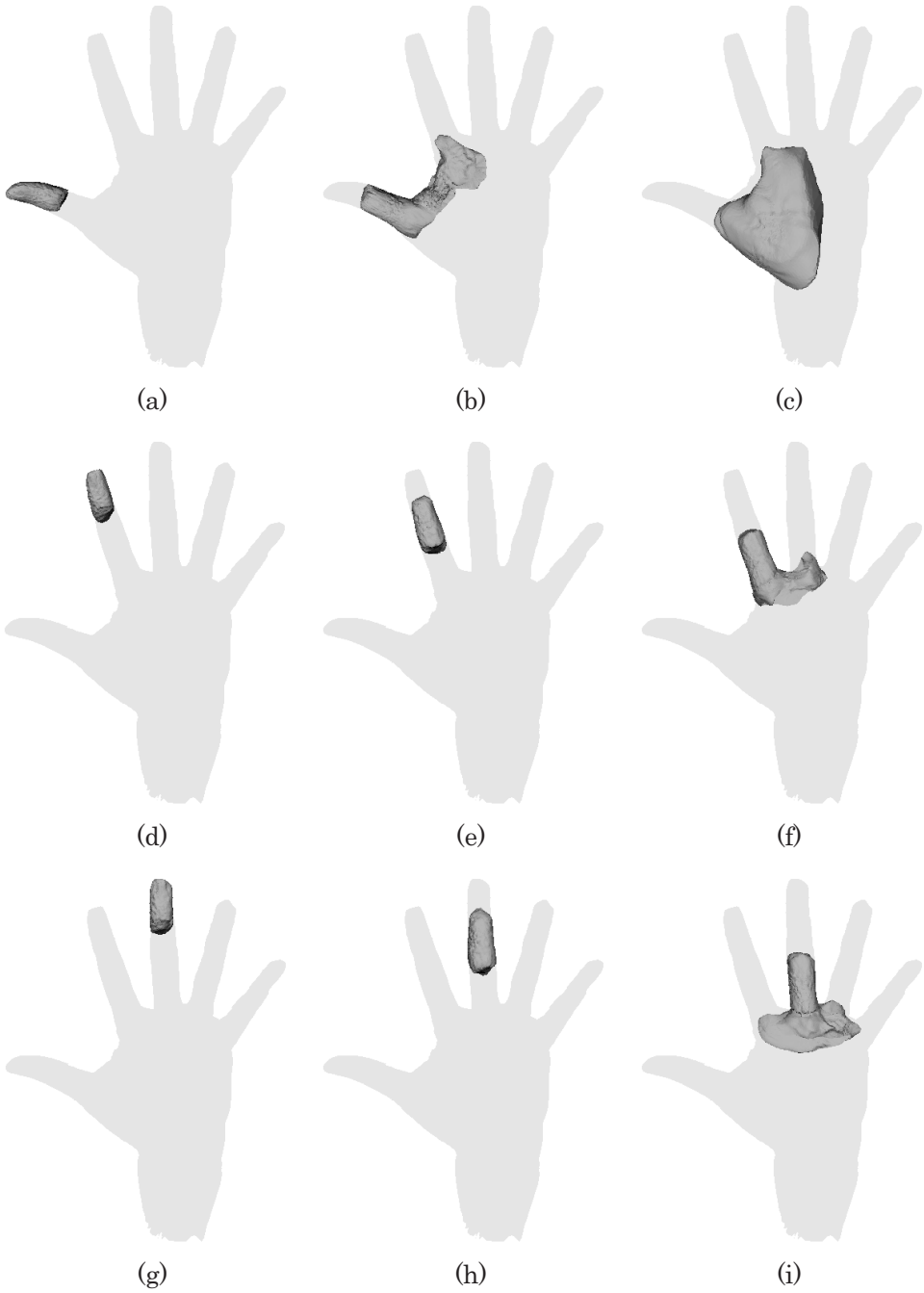

Figure 4.11: Components of hand model.

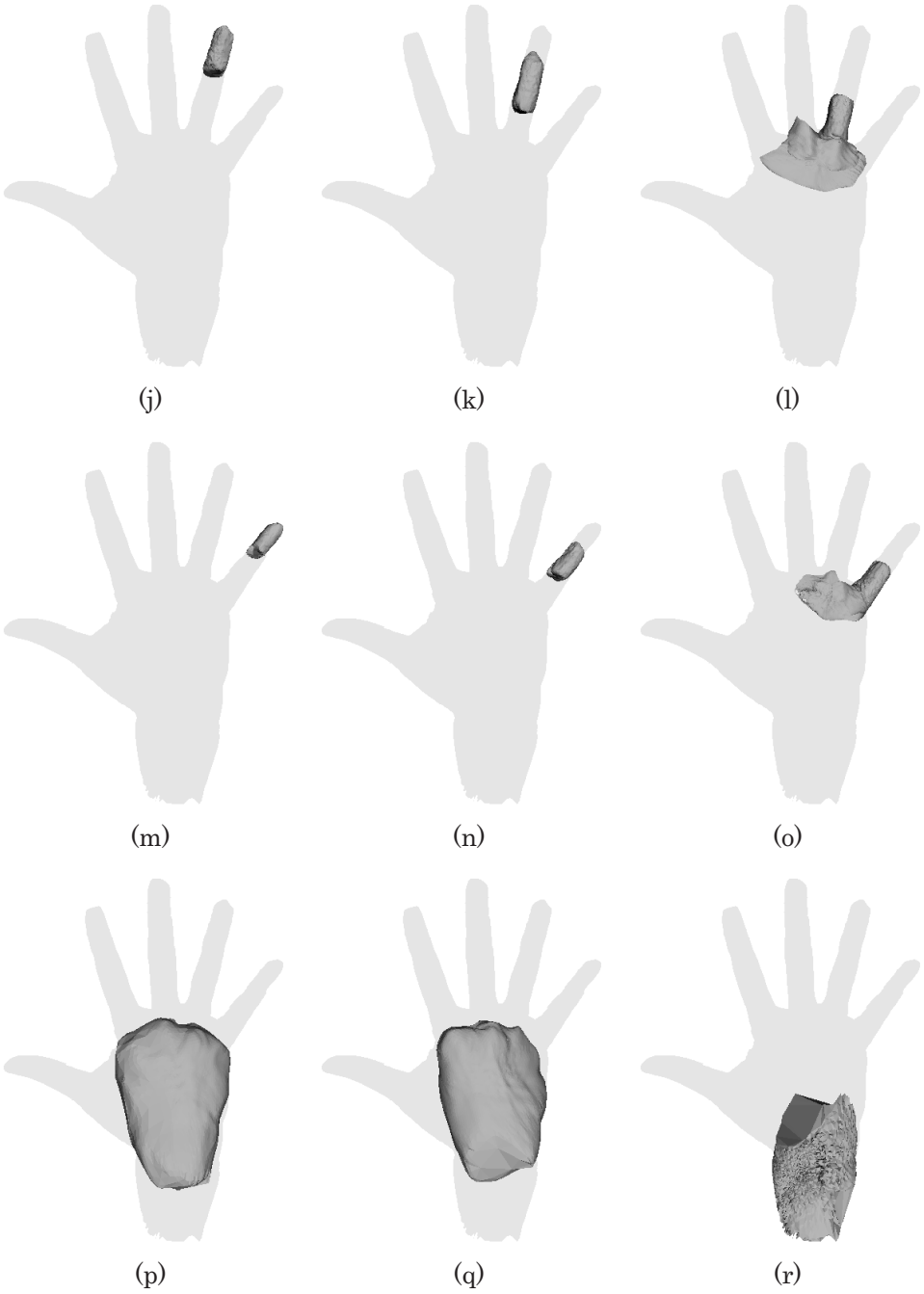

Figure 4.11: (continued)

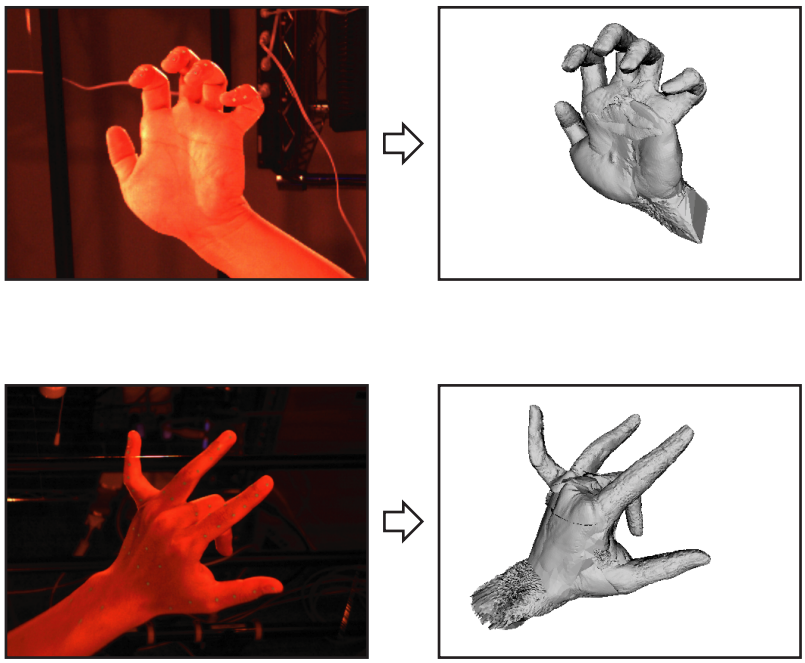

Figure 4.12: Hand model in other postures.

structure, we can estimate the rigid transformations of the components in arbitrary postures and synthesize the shape of the hand.

Several methods of constructing such shape modeling have been proposed for hand [35], human body [13, 1], and others [7, 28].

With conventional light stripe triangulation, it is necessary that the subject maintain the position and the posture of the hand during the measurement, which is several seconds. However, even if the subject makes an effort to maintain the position and the posture of the hand, they would be changed and the acquired shape would be distorted as discussed in Section 3.3.1, and presented in 4.10(a).

Yasumuro et al. [35] made a replica of a hand in a posture by plaster and measured it in order to avoid the distortion. However, this approach can be obstacle to measure the shape of many kinds of object. They also allocate the skeletal model into the reconstructed shape model manually. Ju et al. [13] measure the shape of whole body only in standing posture, segment it into the same components as Douros et al. [4], which is presented in Figure 2.9, and deform the shape model based on generic data which has the skeletal

structure. Starck, Hilton et al. [7, 28] construct skeletal structure (control model) for the scanned data of Michelangelo's David, etc. They also deform the shape in single posture based on the skeletal structure for synthesizing the shapes in arbitrary postures.

Allen et al. [1] measure the shape of human (upper) body in some postures and synthesize the shape in arbitrary posture by integrating them based on the skeletal structure. In order to acquire the shape in some postures without distortion by conventional light structure triangulation, the subject grabbed overhead ropes and makes an effort to maintain the posture.

Meanwhile, the proposed method allows the subject to change its posture freely without degrading the accuracy. Furthermore, the method segment the shape model based on the changing of the shape according to change the posture. Our approach can construct the skeletal structure from the rigid transformations and allocate it into the shape model. Therefore, the proposed method is superior to the other methods in various aspects.

4.5 Conclusion

In this chapter, we proposed the method of segmentation which incorporates the distortion correction by supposing that the subject variously changes its posture during the measurement. For performing the segmentation, the method utilize false shape which appear in distortion correction without segmentation. In order to detect the false shape, the method additionally measures the silhouettes of the subject for some moments, and calculates nonexistent area for each body component of the subject. With the method, we can overcome both 'incompleteness' disadvantage and 'time consuming' disadvantage. We can overcome 'discreteness' disadvantage by reconstructing surface for segmented point-cloud with the method presented in Section 3.4. With above procedure, we can perform human body modeling. We validated through the experiments of measuring pipes, and demonstrated acquired hand model by measuring the real hand.

Chapter 5

Conclusion and Future works

5.1 Conclusion

In this thesis, we discussed the human body modeling of individuals based on three-dimensional shape measurement. When we adopt light stripe triangulation as the method of shape measurement, there are three disadvantages, 'incompleteness', 'time consuming', and 'discreteness'. We presented several methods to tackle these disadvantages in human body modeling.

In Chapter 2, we discussed the principle of light stripe triangulation and its three disadvantages: 'incompleteness', 'time consuming', and 'discreteness'. We also presented the tackling for the disadvantages in conventional human body modeling by supposing that the subject will maintain standing posture during the measurement. However, we can only acquire the human body model in standing posture with this approach. In standing posture, several areas such as under the arms and between the legs are easily occluded and it is difficult to measure such areas. Therefore, 'incompleteness' disadvantage is not completely overcome in conventional human body modeling.

In this thesis, we assumed that human body consists of rigid and almost cylindrical shaped objects, and proposed two approaches for overcoming 'incompleteness' disadvantage. In Chapter 3, we discussed human body modeling with the first approach supposing that the subject will take a posture which is optimal for measuring specific targets in the human body, and will make an effort to maintain the posture during the measurement.

Under this approach, we firstly proposed a method of segmenting the

point-cloud into component of human body. We supposed that the point-cloud forms almost whole human body although it would be incomplete and distorted a little due to the subject's motion during the measurement. By assuming that the size of the subject's body is roughly known, we prepared an articulated body model based on it. The articulated body model is composed of cylinders which represent the components of the subject. The proposed method estimates the posture of the point-cloud by using the articulated body model, and performs the segmentation of the point-cloud based on the articulated body model.

We secondly discussed overcoming 'time consuming' disadvantage under the approach. In order to correct the distortion in point-cloud due to subject's motion, we proposed a method of correcting the distortion in segmented point-cloud of each body component based on its motion during the measurement.

We thirdly discussed overcoming 'discreteness' disadvantage under the approach. Although several methods have been proposed to reconstruct the surface for the point-cloud, these methods would reconstruct the invalid surface for the point-cloud of human body in the concave areas such as the armpits and crotch in standing posture. In order to solve this problem, we proposed a method of reconstructing the surface separately for the each body component, which does not have concave area.

We presented that the proposed method can estimate the posture and perform segmentation for point-cloud which is synthesized and acquired from real human body measurement with a little distortion through the experiment. We also empirically evaluated the distortion in human body measurement with conventional light stripe triangulation and the effectiveness of proposed method which corrects the distortion with the subject's motion.

In Chapter 4, we discussed human body modeling with the second approach supposing that the subject will take many postures during the measurement for getting rid of occluded part in order to make complete human body model by integrating the measurement. The approach supposes that the subject variously changes its posture during the measurement. Therefore, it is supposed that the point-cloud would be catastrophically distorted and it does not form human body.

Since it is difficult to segment seriously distorted point-cloud, we proposed a method of segmentation which incorporates the distortion correction. The method firstly performs correcting distortion without segmentation. Without the segmentation, the method would produce the superfluous shape, false

shape. The method secondly detects the false shape by assuming that every body component does not change its shape in changing posture of the subject. The points which are not detected as false shape are to be segmented into the body component.

We presented the efficiency of the proposed method through the experiment of measuring the actually rigid moving objects and real human hand as substitute for the human body.

5.2 Future works

Motion acquisition In this thesis, we didn't discuss the motion acquisition of body components so much. We utilize an easy and accurate method for acquiring the motion of the body components by putting some markers on each body component as discussed in 3.6.1. Putting the markers enables us to measure its three-dimensional position by stereo vision (just triangulation) and we can estimate rigid motion of the body components based on markers' position. However, human body is not texture-less. The skin has a little texture such as nevus. If we can utilize such texture, we will be able to acquire the motion of the body components without putting markers.

There is yet another possibility that we estimate the motion of the body components from acquired point-cloud itself. We assumed that every body component would not change its shape in this thesis. Even if we have a huge amount of point-cloud, there is consistency of the shape based on the assumption. By taking advantage of the consistency, we will be able to acquire distortion-free shape and the motion of each body component simultaneously.

Deformation analysis Although the approach discussed in Chapter 3 has the merit that we can acquire accurate human body model which can describe the deformation due to the muscle contractions in the posture which the subject made during the measurement, it has the demerit that the acquired human body model can only present the shape in the posture. Meanwhile, the approach discussed in Chapter 4 has the merit that the acquired human body model can describe the shape in various postures however it has the demerit that the acquired model cannot describe the deformation of the body components due to the muscle contractions since we assumed that the body components are rigid.

In order to decide which approach we shall adopt, it is necessary to compare the desired accuracy with the degree of deformation due to the muscle contractions. We will be able to assess the deformation due to the muscle contractions by performing the human body modeling with the approach discussed in Chapter 3 in various postures. If we can acquire the model of the deformation in each component from such assessment, it will be able to extend the approach discussed in Chapter 4 for constructing the human body model which can describe the shape in various postures with the deformation in body components.

Human body measurement with wearing clothes Including the methods discussed in this thesis, conventional human body modeling based on measuring individuals would suppose that the subject is undressed in order to measure the shape of its skin directly. However, it is clear that this supposition would be mental burden for the subject and it would be one of the obstacles to popularize measuring individuals. Therefore, it is desired that some technique is developed to realize the accurate shape measurement of the human body with wearing the clothes.

Extend other methods of shape measurement In this thesis, although we adopted light stripe triangulation for measuring the shape of human body, there are still many methods of measuring three-dimensional shape. For instance, the computed tomography imaging (CT scan, MRI, etc.) is also frequently used in medical fields. Including such method, many methods of measuring the three-dimensional shape takes a certain time. When we utilize such method, there are also the problems principally similar to light stripe triangulation. I believe that the discussion in this thesis will also contribute to solve problems in these methods.

Bibliography

[1] Brett Allen, Brian Curless, and Zoran Popovic. Articulated body deformation from range scan data. *ACM Trans. Graph.*, 21(3):612–619, 2002.

[2] Nina Amenta, Marshall W. Bern, and Manolis Kamvysselis. A new voronoi-based surface reconstruction algorithm. In *SIGGRAPH*, pages 415–421, 1998.

[3] Zouhour Ben Azouz, Marc Rioux, and Richard Lepage. 3d description of the human body shape using karhunen-loeve expansion. *International Journal of Information Technology*, 8(2):26–35, 2002.

[4] Ioannis Douros, Laura Dekker, and Bernard F. Buxton. An improved algorithm for reconstruction of the surface of the human body from 3d scanner data using local b-spline patches. In *Proc. of the IEEE International Workshop on Modelling People*, pages 29–36, 1999.

[5] Tsung-Pao Fang and Les A. Piegl. Delaunay triangulation in three dimensions. *IEEE Computer Graphics and Applications*, 15(5):62–69, 1995.

[6] Kazuyuki Hattori and Yukio Sato. Accurate rangefinder with laser pattern shifting. In *ICPR(3)*, pages 849–853, 1996.

[7] Adrian Hilton, Jonathan Starck, and Gordon Collins. From 3d shape capture to animated models. In *1st International Symposium on 3D Data Processing Visualization and Transmission (3DPVT 2002)*, pages 246–257, 2002.

[8] Loram ID, Kelly SM, and Lakie M. Human balancing of an inverted pendulum: is sway size controlled by ankle impedance? *J. Physiology*, 532(3):879–891, 2001.

[9] Cyberware Inc. Whole body x 3d scanner. http://www.cyberware.com/.

[10] Hamamatsu Inc. Bodyline scanner. http://www.hpk.co.jp/.

[11] Vitronic Inc. Vitus smart xxl. http://www.vitronic.com/.

[12] VOXELAN Inc. Voxelan. http://www.voxelan.co.jp/.

[13] Xiangyang Ju and J. Paul Siebert. Individualising human animation models. In *Proc. Eurographics*, 2001.

[14] XIANGYANG JU, NAOUFEL WERGHI, and J. PAUL SIEBERT. Automatic segmentation of 3d human body scans. In *IASTED International Conference on Computer Graphics and Imaging 2000 (CGIM 2000)*, pages 19–23, 2000.

[15] Adam G. Kirk, James F. O'Brien, and David A. Forsyth. Skeletal parameter estimation from optical motion capture data. In *IEEE Computer Society Conference on Computer Vision and Pattern Recognition (CVPR)*, pages 782–788, 2005.

[16] Worhty N. Martin and J.K. Aggarwal. Volumetric description of objects from multiple views. *IEEE Trans. on Pattern Analysis and Machine Intelligence.*, 5(2):150–158, 1983.

[17] Tsukasa Matsuoka, Kenji Ueda, and Masayuki Hayano. Solid model reconstruction from unorganized points with a marching lattice points method and local operations. *IPSJ Journal*, 40(5):2377–2386, 1999. (in Japanese).

[18] Dimitris Metaxas, Eunyoung Koh, and Norman I. Badler. Multi-level shape representation using global deformations and locally adaptive finite elements. *International Journal of Computer Vision*, 25(1):49–61, 1997.

[19] James F. O'Brien, Robert E. Bodenheimer, Gabriel J. Brostow, and Jessica K. Hodgins. Automatic joint parameter estimation from magnetic

motion capture data. In *Proceedings of the Graphics Interface*, pages 53–60, 2000.

[20] Yusuke Oike, Makoto Ikeda, and Kunihiro Asada. A cmos image sensor for high-speed active range finding using column-parallel time-domain adc and position encoder. *IEEE Trans. Electron Devices*, 50(1):152–158, 2003.

[21] Masatoshi Okutomi and Takeo Kanade. A multi-baseline stereo. *IEEE Trans. on Pattern Analysis and Machine Intelligence.*, 15(4):353–363, 1993.

[22] Nobuyuki Otsu. A threshold selection method from gray-level histograms. *IEEE Trans. Syst. Man & Cybern.*, 9(1):62–69, 1979.

[23] W.H. Press, B.P. Flannery, S.A. Teukolsky, and W.T. Vetterling. *Numerical Recipes in C, the Art of Scientific Computing, Second Edition.* Cambridge University Press, 1992.

[24] Maurice Ringer and Joan Lasenby. A procedure for automatically estimating model parameters in optical motion capture. *Image Vision Comput.*, 22(10):843–850, 2004.

[25] K. M. Robinette and Hans Daanen. The caesar project: A 3-d surface anthropometry survey. In *2nd International Conference on 3D Digital Imaging and Modeling (3DIM '99)*, pages 380–386, 1999.

[26] Hideki Sato and Kinya Fujita. Role distribution between ankle joint stiffness and stretch reflex in human postural control. *Trans. of the Society of Instrument and Control Engineers*, 35(5):600–605, 1999. (in Japanese).

[27] C. Sinlapeecheewa and K. Takamasu. 3d profile measurement by color pattern projection and system calibration. In *Proc.of ICITf02*, pages 405–410, 2002.

[28] Jonathan Starck, Gordon Collins, Raymond Smith, Adrian Hilton, and John Illingworth. Animated statues. *Machine Vision and Applications.*, 14(4):248–259, 2003.

[29] Shinichi Takasaki, Shohei Hayashi, Taishin Nomura, and Shunsuke Sato. A musculo-skeletal model of human quiet upright postural control. MBE2001-16 101-93, IEICE, 2001. (in Japanese).

[30] Toshio Ueshiba and Fumiaki Tomita. A factorization method for projective and euclidean reconstruction from multiple perspective views via iterative depth estimation. In *5th European Conference on Computer Vision*, pages 296–310, 1998.

[31] Piet Vuylsteke and André Oosterlinck. Range image acquisition with a single binary-encoded light pattern. *IEEE Trans. Pattern Anal. Mach. Intell.*, 12(2):148–164, 1990.

[32] David A. Winter, Aftab E. Patla, Francois Prince, Milad Ishac, and Krystyna Gielo-Perczak. Stiffness control of balance in quiet standing. *J. Neurophysiol*, 80(3):1211–1221, 1998.

[33] David A Winter, Aftab E Patla, Shirley Rietdyk, and Milad G Ishac. Ankle muscle stiffness in the control of balance during quiet standing. *J. Neurophysiol*, 85(6):2630–2633, 2001.

[34] Robert J. Woodham. Photometric method for determining surface orientation from multiple images. *Journal of Optical Engineering.*, 19(1):138–144, 1980.

[35] Yoshihiro Yasumuro, Qian Chen, and Kunihiro Chihara. Three-dimensional modeling of the human hand with motion constraints. *Image Vision Comput.*, 17(2):149–156, 1999.

[36] Zhengyou Zhang. A flexible new technique for camera calibration. *IEEE Trans. Pattern Anal. Mach. Intell.*, 22(11):1330–1334, 2000.

List of Publications

Journal Articles

1. Takuya FUNATOMI, Masaaki IIYAMA, Koh KAKUSHO, Michihiko MINOH, "Light stripe triangulation for multiple moving objects," conditionally accepted to IEICE Trans. on Information and Systems. (In Japanese)

2. Takuya FUNATOMI, Masaaki IIYAMA, Koh KAKUSHO, Michihiko MINOH, "Accurate 3D scanning of trunk swaying human body parts," IEICE Trans. on Information and Systems, Vol.J88-D2, No.8, pp.1530-1538, 2005. (In Japanese)

3. Takuya FUNATOMI, Isao MORO, Shinobu MIZUTA, Michihiko MINOH, "Surface reconstruction from point cloud of human body by using clustering," IEICE Trans. on Information and Systems, Vol.J87-D2, No.2, pp.649-660, 2004. (In Japanese)
   Takuya FUNATOMI, Isao MORO, Shinobu MIZUTA, Michihiko MINOH, "Surface reconstruction from point cloud of human body by clustering," Systems and Computers in Japan, Vol.37, No.11, pp.44-56, 2006.

Refereed Conference Presentations

1. Takuya FUNATOMI, Masaaki IIYAMA, Koh KAKUSHO, Michihiko MINOH, "Light stripe triangulation for multiple of moving rigid objects," Submitted to IEEE Computer Society Conference on Computer Vision and Pattern Recognition (CVPR).

2. Takuya FUNATOMI, Masaaki IIYAMA, Koh KAKUSHO, Michihiko MIHOH, "3D Shape Reconstruction of Trunk Swaying Human Body Segments," Articulated Motion and Deformable Objects: 4th International Conference (AMDO 2006), Lecture Notes in Computer Science (LNCS) Vol.4069 pp.100-109, 2006.

3. Takuya FUNATOMI, "3D shape and structure modeling by measuring individual human body," Doctor Student Conference, Association of Pacific Rim Universities (APRU DSC2006), 2006.

4. Takuya FUNATOMI, Masaaki IIYAMA, Koh KAKUSHO, Michihiko MIHOH, "Accurate 3D scanning of trunk swaying human body," Meeting on Image Recognition and Understanding 2004 (MIRU2004), Vol.I, pp.565-570, 2004. (In Japanese)

Conference Presentations

1. Kosuke OSHIMA, Takuya FUNATOMI, Masaaki IIYAMA, Koh KAKUSHO, Michihiko MINOH, "Direct manipulation of virtual object using real object in virtual studio," 2006 IEICE General Conference, A-16-24, p.286, 2006. (In Japanese)

2. Naoki OKADA, Takuya FUNATOMI, Masaaki IIYAMA, Koh KAKUSHO, Michihiko MINOH, "Motion modeling from image sequence based on the laws of motion," 2006 IEICE General Conference, A-16-11, p.273, 2006. (In Japanese)

3. Takuya FUNATOMI, Masaaki IIYAMA, Koh KAKUSHO, Michihiko MIHOH, "Analysis of trunk sway for human balancing by stereo measurement," Forum on Information Technology 2004 (FIT 2004), No.3-K008, pp.407-408, 2004. (In Japanese)

4. Takuya FUNATOMI, Isao MORO, Masaaki IIYAMA, Michihiko MINOH, "Surface reconstruction from Point Cloud of Human Body by Using Clustering," TECHNICAL REPORT OF IEICE, Vol.MVE-2002-133, pp.53-56, 2003. (In Japanese)

5. Takuya FUNATOMI, Masaaki IIYAMA, Shinobu MIZUTA, Michihiko MINOH, "Generation of Trajectory for Local Self-intersection Free 3D

Metamorphosis between Patch Models," Forum on Information Technology 2002 (FIT 2002), No.3-J42, pp.285-286, 2002. (In Japanese)

6. Shinobu MIZUTA, Hidekuni ANNAKA, Takuya FUNATOMI, Michihiko MINOH, "Growth Representation of Human Embryos by 3 Dimensional Mesh Morphing Considering Trajectories," IPSJ SIG Notes Graphics and CAD, No.104, pp.41-46, 2001. (In Japanese)